Symbol-by-Symbol Maximum Likelihood Detection for Cooperative Molecular Communication

Yuting Fang, *Student Member, IEEE*, Adam Noel, *Member, IEEE*, Nan Yang, *Senior Member, IEEE*, Andrew W. Eckford, *Senior Member, IEEE*, and Rodney A. Kennedy, *Fellow, IEEE*

***Abstract*—In this paper, symbol-by-symbol maximum likelihood (ML) detection is proposed for a cooperative diffusion-based molecular communication (MC) system. In this system, the transmitter (TX) sends a common information symbol to multiple receivers (RXs) and a fusion center (FC) chooses the TX symbol that is more likely, given the likelihood of its observations from all RXs. The transmission of a sequence of binary symbols and the resultant intersymbol interference are considered in the cooperative MC system. Three ML detection variants are proposed according to different RX behaviors and different knowledge at the FC. The system error probabilities for two ML detector variants are derived, one of which is in closed form. The optimal molecule allocation among RXs to minimize the system error probability of one variant is determined by solving a joint optimization problem. Also for this variant, the equal distribution of molecules among two symmetric RXs is analytically shown to achieve the local minimal error probability. Numerical and simulation results show that the ML detection variants provide lower bounds on the error performance of simpler, non-ML cooperative variants and demonstrate that these simpler cooperative variants have error performance comparable to ML detectors.**

***Index Terms*—Molecular communication, multi-receiver cooperation, symbol-by-symbol maximum likelihood detection, error performance, optimization**

I. Introduction

Molecular communication (MC) has been heralded as one of the most promising paradigms to implement communication in bio-inspired nanonetworks, due to the potential benefits of bio-compatibility and low energy consumption [2]. In MC, the information transmission between devices is realized through the exchange of molecules. Since no source of external energy is required for free diffusion, it is the simplest molecular propagation mechanism. One of the primary challenges posed by diffusion-based MC is that its reliability rapidly decreases when the transmitter (TX)-receiver (RX) distance increases. A naturally-inspired approach, which also makes use of the envisioned collaboration between nanomachines, is allowing multiple RXs to share information for cooperative detection. Often, cells or organisms share common information to achieve a specific task, e.g., calcium (Ca^{2+}) signaling [3].

The majority of existing MC studies have focused on the modeling of a single-RX MC system [2]. Recent studies, e.g., [4–7], have expanded the single-RX MC system to a multi-RX MC system. Although these studies stand on their own merit, they did not establish the potential of *active cooperation* among multiple RXs to determine a TX's intended symbol sequence in a multi-RX MC system, i.e., the RXs do not actively share their available information to determine the transmitted information. To address this gap, our work in [8–10] analyzed the error performance of a cooperative diffusion-based MC system where a fusion center (FC) device combines the binary decisions of distributed RXs to improve the detection of a TX's symbols.

In other fields of communications, e.g., wireless communications, the maximum likelihood (ML) detector is commonly used to optimize detection performance [11, Ch, 5]. In the MC domain, the ML sequence detector has been considered for optimality in several studies, e.g., [12, 13]. However, the high complexity of sequence detection is a significant barrier to implementation in the MC domain, even when applying simplified algorithms.

The (suboptimal) symbol-by-symbol ML detector requires less computational complexity than the ML sequence detector. Motivated by this, [14–16] considered symbol-by-symbol ML detection at a single RX for MC. Recently, [17–19] considered cooperative ML detection for MC. However, in [17, 18] the RXs communicate with an FC but do not detect information from a TX. Also, in [18, 19] the FC makes a single decision about the presence of an abnormality, such that there is only one information symbol and no symbol-by-symbol detection.

In this paper, we present symbol-by-symbol ML detection for a cooperative diffusion-based MC system, based on [8–10], which consists of one TX, K RXs, and an FC. The significance of this paper is that our results provide lower bounds on the error performance that can be achieved by the detectors considered in [8–10]. In our proposed system, the transmission of each information symbol from the TX to the FC via the RXs is completed in two phases, as shown in Fig. 1. In the first phase, the TX sends a symbol that is observed by all RXs. In the second phase, the RXs send their detected information to the FC and the FC chooses the TX symbol that is more likely, given the likelihood of its observations from all RXs.

Since binary symbols are the easiest to transmit and detect [20], and we assume that the TX needs to send multiple bits of information in order to execute some complex task (such as disease localization), we consider the transmission of a *sequence* of binary symbols and account for the resultant ISI due to previous symbols at the TX and the RXs in the design and analysis of the cooperative MC system. The results of this paper could be applied to health and environmental

This work was presented in part at the IEEE ICC 2018 [1].

Y. Fang, N. Yang, and R. A. Kennedy are with the Research School of Electrical, Energy, and Materials Engineering, Australian National University, Canberra, ACT 2600, Australia (e-mail: {yuting.fang, nan.yang, rodney.kennedy}@anu.edu.au).

A. Noel is with the School of Engineering, University of Warwick, Coventry, CV4 7AL, UK (e-mail: adam.noel@warwick.ac.uk).

A. W. Eckford is with the Department of Electrical Engineering and Computer Science, York University, Toronto, ON M3J 1P3, Canada (e-mail:aeckford@yorku.ca)

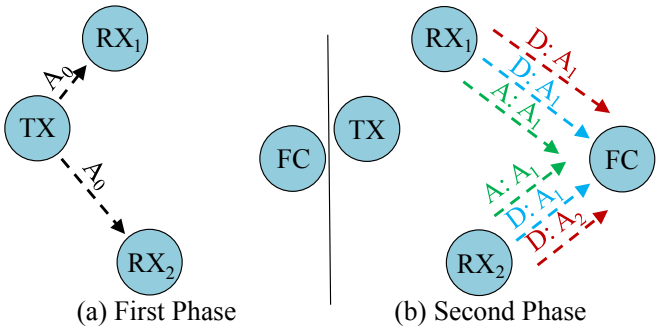

Fig. 1. An example of a cooperative MC system with 2 RXs. The transmission from the TX to the RXs is represented by black dashed arrows. "D" and "A" denotes the RXs making decisions and amplifying observations, respectively, and A_k denotes the type of released molecule. The transmission from the RXs to the FC in MD-ML, SD-ML, and SA-ML are represented by red, blue, and green arrows, respectively.

TABLE I
VARIANTS OF ML DETECTORS

Acronym	Relaying at RXs	Molecule Type used in RXs	Behavior at FC	Complexity Comparison
MD-ML	DF	Multiple	ML Detection	MD-ML >SD-ML >SA-ML
SD-ML	DF	Single	ML Detection	
SA-ML	AF	Single	ML Detection	

monitoring and drug delivery scenarios. In these scenarios, the TX can be a nanomachine that transmits environmental sensor values, e.g., concentration, blood pressure, and temperature, or broadcasts the location of a target site. To the best of the authors' knowledge, combined with our previous work in [1], this work is the *first* to apply *symbol-by-symbol* ML detection to a cooperative MC system with *multiple* communication phases. Although the system topology design and general communication processes can be adapted for traditional cooperative communications, our results cannot be directly applied to traditional cooperative communications due to unique ISI, the propagation channels, and the signal types in this work.

In this paper, we present three symbol-by-symbol ML detectors: 1) decode-and-forward (DF) with multi-molecule-type and ML detection at the FC (MD-ML), 2) DF with single-molecule-type and ML detection at the FC (SD-ML), and 3) Amplify-and-forward (AF) with single-molecule-type and ML detection at the FC (SA-ML). We summarize these variants in Table I. We design the detectors according to different relaying modes and numbers of types of molecules available at RXs. These variants use either DF relaying or AF relaying and multi-type or single-type molecules. Generally, DF outperforms AF [21] and multi-type outperforms single-type molecules, but assumptions of AF and single-type molecules are more realistic in biological environments. ML detection in the current symbol interval requires knowing the previously-transmitted symbols by the TX (and by all RXs for DF). For convenience, we refer to the FC-estimated previous symbols as *local history* and the perfect knowledge of the previous symbols as *genie-aided history*. Our major contributions are summarized as follows:

1) We present novel symbol-by-symbol ML detection designs for the cooperative MC system with all detector variants, i.e., SD-ML, MD-ML, and SA-ML. For practicality, we consider the FC chooses the current symbol using its *local history* and design the methods for the FC to obtain the local history. We also derive the likelihood of observations for all detectors.
2) We derive analytical expressions for the system error probability for SD-ML and SA-ML using the assumption of *genie-aided history*. This assumption leads to tractable error performance analysis. The error probabilities for SD-ML with $K = 1$ and SA-ML are given in closed form. The error performance of MD-ML is mathematically intractable.
3) We determine the optimal molecule allocation among RXs to minimize the system error probability of SD-ML, which provides a lower bound on the system error probability that can be achieved in practice. To this end, we formulate and solve a joint optimization problem in terms of molecule allocation and a constant threshold. In this problem, the objective function is the closed-form approximation of error probability of SD-ML since there is no closed-form expression for the error probability of SD-ML. We also analytically prove that the equal distribution of molecules among two symmetric RXs achieves the local minimal error probability of SD-ML.
4) We validate the accuracy of our analytical expressions of error probability via a particle-based simulation method where we track the motions of molecules over time due to diffusion. Using simulation and numerical results, we also demonstrate the FC's effectiveness in estimating the previously-transmitted symbols and confirm the effectiveness of our optimization method.

In contrast to our preliminary work in [1], which only presents ML detection design of SD-ML in a symmetric topology, and did not derive the system error probability, this paper presents two additional detector variants, i.e., MD-ML and SA-ML, relaxes the constraint of symmetric topology, and derives and optimizes the system error probability.

Although the ML detection requires high complexity, our system could be implemented in a practical scenario for the following reasons: 1) We consider relatively simple RXs with an energy detector or a signal amplifier. The computations required at the RXs can be implemented at the molecular level [22]; 2) We keep the relatively high complexity required for ML detection at the FC since it could have a direct interface with the macroscopic world and easier access to computational resources; 3) The memory required at the FC may be implemented by synthesizing a memory unit inside the FC [23]; 4) A modified cell and a synthetic oscillator can be introduced into devices to release specific molecules and control the timing of molecule release [24].

Notations: We use the following notations: $\Pr(\cdot)$ denotes probability. $\lfloor x \rfloor$ denotes the greatest integer that is less than or equal to x, $\lceil x \rceil$ denotes the smallest integer that is greater than or equal to x, and $\lfloor \cdot \rceil$ denotes the nearest integer. $\log(\cdot)$ is the natural logarithm, $\mathrm{erf}(\cdot)$ is the error function, and $\exp(\cdot)$ is the exponential function. $|\cdot|$ is the cardinality of a set.

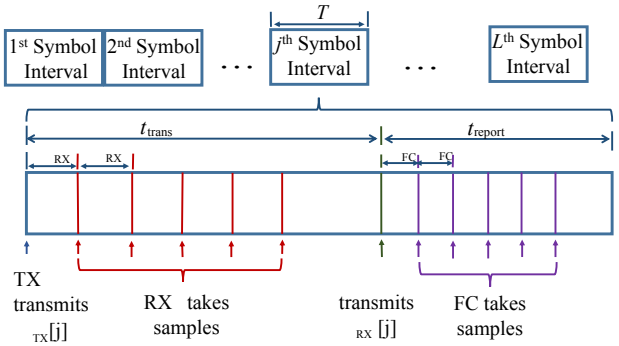

Fig. 2. An example of the timing schedule for the system with $M_{\text{RX}} = 5$ and $M_{\text{FC}} = 5$.

II. System Model and Preliminaries

In this section, we present the system model (i.e., physical environment and general behaviors of devices) for the cooperative MC system and some preliminary results that are needed in Section III. We will describe specific behaviors of the RXs and the FC for the ML detector variants in Section III.

A. System Model

We consider a cooperative MC system in unbounded three-dimensional space. An example of the system is illustrated in Fig. 1. We assume that all RXs and the FC are passive spherical observers. Accordingly, we denote V_{RX_k} and r_{RX_k} as the volume and radius of the kth RX, RX_k, respectively, where $k \in \{1, 2, \ldots, K\}$. We also denote V_{FC} and r_{FC} as the volume and radius of the FC, respectively. We use the terms "sample" and "observation" interchangeably to refer to the number of molecules observed by a RX or the FC at some time t and assume each observation is independent of each other[1]. The symbol interval time from the TX to the FC is given by $T = t_{\text{trans}} + t_{\text{report}}$, where t_{trans} is the transmission interval time from the TX to the RXs and t_{report} is the report interval time from the RXs to the FC.

In the following, we describe the timing schedules and general behaviors of the TX, the RXs, and the FC. An example of the timing schedule for the system is shown in Fig. 2. Various methods can be adopted to achieve time synchronization[2] among nanomachines, e.g., [25, 26].

TX: At the beginning of the jth symbol interval, i.e., $(j-1)T$, the TX transmits $W_{\text{TX}}[j]$. The TX transmits $W_{\text{TX}}[j]$ to the RXs over the diffusive channel via type A_0 molecules which diffuse independently. The TX uses ON/OFF keying [20] to convey information, i.e., the TX releases S_0 molecules of type A_0 to convey information symbol "1" with probability $\Pr(W_{\text{TX}}[j] = 1) = P_1$, but no molecules to convey information symbol "0". The TX then keeps silent until the start of the $(j+1)$th symbol interval. We denote L as the number of symbols transmitted by the TX. We define $\mathbf{W}_{\text{TX}}^{l} = \{W_{\text{TX}}[1], \ldots, W_{\text{TX}}[l]\}$ as an l-length subsequence of the symbols transmitted by the TX, where $l \leq L$. Throughout the paper, W is a single symbol and $\mathbf{W}$ is a vector of symbols. We do not consider channel codes for this system since the required encoder and the decoder may not be practical for MC systems [2, 27].

RX: Each RX_k observes type A_0 molecules over the $\text{TX} - \text{RX}_k$ link and takes M_{RX} samples[3] in each symbol interval at the same times. The time of the mth sample by each RX in the jth symbol interval is given by $t_{\text{RX}}(j, m) = (j-1)T + m\Delta t_{\text{RX}}$, where Δt_{RX} is the time step between two successive samples by each RX, $m \in \{1, 2, \ldots, M_{\text{RX}}\}$. The RXs operate in half-duplex mode, such that they do not receive the information and report their decisions at the same time. This is because half-duplex mode is more appropriate in a biological environment since it requires lower computational complexity than full-duplex mode. At the time $(j-1)T + t_{\text{trans}}$, each RX transmits molecules via a diffusion-based channel to the FC. For MD-ML and SD-ML, each RX detects with a relatively simple *energy* detector [13]. We denote $\hat{W}_{\text{RX}_k}[j]$ as RX_k's binary decision on the jth transmitted symbol. Based on the energy detector, RX_k makes decision $\hat{W}_{\text{RX}_k}[j] = 1$ if $s_k[j] \geq \xi_{\text{RX}_k}$, otherwise $\hat{W}_{\text{RX}_k}[j] = 0$, where $s_k[j]$ is the value of the realization of $S_{\text{ob}}^{\text{RX}_k}[j]$ and ξ_{RX_k} is the constant detection threshold at RX_k, independent of $\mathbf{W}_{\text{TX}}^{j-1}$. We define $\hat{\mathbf{W}}_{\text{RX}_k}^{l} = \left\{\hat{W}_{\text{RX}_k}[1], \ldots, \hat{W}_{\text{RX}_k}[l]\right\}$ as an l-length subsequence of RX_k's binary decisions.

FC: The FC takes the $\tilde{m}$th sample in the jth symbol interval at $t_{\text{FC}}(j, \tilde{m}) = (j-1)T + t_{\text{trans}} + \tilde{m}\Delta t_{\text{FC}}$, where Δt_{FC} is the time step between two successive samples by the FC and $\tilde{m} \in \{1, 2, \ldots, M_{\text{FC}}\}$. We denote $\hat{W}_{\text{FC}}[j]$ as the FC's decision on the jth symbol transmitted by the TX. We define $\hat{\mathbf{W}}_{\text{FC}}^{l} = \left\{\hat{W}_{\text{FC}}[1], \ldots, \hat{W}_{\text{FC}}[l]\right\}$ as an l-length subsequence of the FC's decisions on the symbols transmitted by the TX. We denote $\hat{W}_{\text{FC}_k}[j]$ as the FC's estimated binary decision of RX_k on the jth transmitted symbol. We define $\hat{\mathbf{W}}_{\text{FC}_k}^{l} = \left\{\hat{W}_{\text{FC}_k}[1], \ldots, \hat{W}_{\text{FC}_k}[l]\right\}$ as the FC's estimate of the first l binary decisions by RX_k.

B. Preliminaries

In this subsection, we establish some preliminary results for a $\text{TX} - \text{RX}_k$ link and a $\text{RX}_k - \text{FC}$ link. We first evaluate the probability $P_{\text{ob}}^{(\text{TX},\text{RX}_k)}(t)$ of observing a given type A_0 molecule, emitted from the TX at $t = 0$, inside V_{RX_k} at time t. Based on [28, Eq. (27)], we write $P_{\text{ob}}^{(\text{TX},\text{RX}_k)}(t)$ as

$$P_{\text{ob}}^{(\text{TX},\text{RX}_k)}(t) = \frac{1}{2}\left[\text{erf}\left(\tau_1\right) + \text{erf}\left(\tau_2\right)\right] - \frac{\sqrt{D_0 t}}{d_{\text{TX}_k}\sqrt{\pi}}\left[\exp\left(-\tau_1^2\right) - \exp\left(-\tau_2^2\right)\right], \quad (1)$$

where $\tau_1 = \frac{r_{\text{RX}_k} + d_{\text{TX}_k}}{2\sqrt{D_0 t}}$, $\tau_2 = \frac{r_{\text{RX}_k} - d_{\text{TX}_k}}{2\sqrt{D_0 t}}$, D_0 is the diffusion coefficient of type A_0 molecules in m^2/s, d_{TX_k} is the distance

[1] Intuitively, we consider the time between samples sufficiently large and the distances between the RXs sufficiently large for all individual observations to be independent. The validity of assuming independence will be demonstrated by the excellent agreement between analytical and simulation results in Section VI.

[2] All RXs may not be perfectly synchronized. We make the assumption of identical sampling times at all RXs to get a bound on the best error performance achievable by a practical cooperative MC system.

[3] We consider multiple samples at the RXs and the FC in each symbol interval to improve the detection performance.

TABLE II
ILLUSTRATION OF THE FC'S LOCAL HISTORY

Interval	The FC's decisions	The FC's local history
1	$\hat{W}_{\text{FC}}[1]$ and $\hat{W}_{\text{FC}_k}[1]$	No History
2	$\hat{W}_{\text{FC}}[2]$ and $\hat{W}_{\text{FC}_k}[2]$	$\hat{W}_{\text{FC}}[1]$ and $\hat{W}_{\text{FC}_k}[1]$
$\vdots$	$\vdots$	$\vdots$
L	$\hat{W}_{\text{FC}}[L]$ and $\hat{W}_{\text{FC}_k}[L]$	$\hat{W}_{\text{FC}}[L-1],\ldots,\hat{W}_{\text{FC}}[1]$ and $\hat{W}_{\text{FC}_k}[L-1],\ldots,\hat{W}_{\text{FC}_k}[1]$

between the TX and RX_k in m. We denote the sum of M_{RX} samples by RX_k in the jth symbol interval by $S_{\text{ob}}^{\text{RX}_k}[j]$. As discussed in [29, 30], $S_{\text{ob}}^{\text{RX}_k}[j]$ can be accurately approximated by a Poisson random variable (RV). The mean of $S_{\text{ob}}^{\text{RX}_k}[j]$ is then given by

$$\bar{S}_{\text{ob}}^{\text{RX}_k}[j]=\sum_{i=1}^{j} S_0 W_{\text{TX}}[i] \sum_{m=1}^{M_{\text{RX}}} P_{\text{ob}}^{(\text{TX},\text{RX}_k)}((j-i)\,T+m\Delta t_{\text{RX}})\,. \quad (2)$$

We denote $P_{\text{ob},k}^{(\text{RX}_k,\text{FC})}(t)$ as the probability of observing a given A_k molecule, emitted from the center of RX_k at $t=0$, inside V_{FC} at time t. We obtain $P_{\text{ob},k}^{(\text{RX}_k,\text{FC})}(t)$ by replacing r_{RX_k}, d_{TX_k}, and D_0 with r_{FC}, d_{FC_k}, and D_k, respectively, where D_k is the diffusion coefficient of type A_k molecules in m^2/s and d_{FC_k} is the distance between RX_k and the FC in m.

III. ML DETECTION DESIGN AND DERIVATION

In this section, we design and derive three symbol-by-symbol ML detectors. Throughout this section, the FC uses its *local* history to choose the current symbol, i.e., the FC evaluates the likelihood of the observations $\hat{\mathbf{W}}_{\text{FC}}^{j-1}$ and $\hat{\mathbf{W}}_{\text{FC}_k}^{j-1}$ ($\hat{\mathbf{W}}_{\text{FC}_k}^{j-1}$ is not needed for SA-ML) in the jth symbol interval, as shown in Table II, where $k\in\{1,2,\ldots,K\}$. Using the local history at the FC, we formulate the general decision rule of ML detection in the jth interval as

$$\hat{W}_{\text{FC}}[j]=\underset{W_{\text{TX}}[j]\in\{0,1\}}{\text{argmax}}\ \mathcal{L}\left[j|W_{\text{TX}}[j],\hat{\mathbf{W}}_{\text{FC}}^{j-1}\right] \quad (3)$$

or

$$\hat{W}_{\text{FC}}[j]=\underset{W_{\text{TX}}[j]\in\{0,1\}}{\text{argmax}}\ \mathcal{L}\left[j|W_{\text{TX}}[j],\hat{\mathbf{W}}_{\text{FC}}^{j-1},\hat{\mathbf{W}}_{\text{FC}_k}^{j-1}\right], \quad (4)$$

where we define $\mathcal{L}[j|\cdot]\triangleq \Pr(\text{FC's observations in } j\text{th interval}|\cdot)$. Eq. (3) applies to SA-ML and (4) applies to SD-ML and MD-ML. For simplicity, we also write the likelihoods in (3) and (4) as $\mathcal{L}[j]$. In the following, we present the specific behaviors of the RXs and the FC of each ML detector, derive the corresponding $\mathcal{L}[j]$, and compare the complexities of the detectors.

A. MD-ML

Each RX_k in MD-ML transmits type A_k molecules, which can be independently detected by the FC, to report $\hat{W}_{\text{RX}_k}[j]$ to the FC. Similar to the TX, each RX uses ON/OFF keying to report its decision to the FC and the RX releases S_k molecules of type A_k to convey information symbol "1". The FC receives type A_k molecules over the RX_k-FC link and takes M_{FC} samples of each of the K types of molecules transmitted by all RXs in every reporting interval. The FC adds M_{FC} observations for each RX_k-FC link in the jth symbol interval. We denote $S_{\text{ob},k}^{\text{FC,D}}[j]$ as the total number of A_k molecules observed within V_{FC} in the jth symbol interval, due to both current and previous emissions of molecules by RX_k. The TX and RX_k use the same modulation method and the $\text{TX}-\text{RX}_k$ and RX_k-FC links are both diffusion-based. Therefore, like $S_{\text{ob}}^{\text{RX}_k}[j]$, $S_{\text{ob},k}^{\text{FC,D}}[j]$ can also be accurately approximated as a Poisson RV. We denote $\bar{S}_{\text{ob},k}^{\text{FC,D}}[j]$ as the mean of $S_{\text{ob},k}^{\text{FC,D}}[j]$. Values of realizations of $S_{\text{ob},k}^{\text{FC,D}}[j]$ are labeled $\tilde{s}_k[j]$. We assume that the K RX_k-FC links are independent, so the FC has K independent sums $\tilde{s}_k[j]$ from the K RX_k-FC links. The FC chooses the symbol $\hat{W}_{\text{FC}}[j]$ that is more likely, given the joint likelihood of the K sums $\tilde{s}_k[j]$ in the jth interval. We obtain $\mathcal{L}[j]$ by

$$\begin{aligned}\mathcal{L}[j]=\prod_{k=1}^{K}\Bigg[&\Pr\left(\hat{W}_{\text{RX}_k}[j]=1|W_{\text{TX}}[j],\hat{\mathbf{W}}_{\text{FC}}^{j-1}\right)\\&\times\Pr\left(S_{\text{ob},k}^{\text{FC,D}}[j]=\tilde{s}_k[j]|\hat{W}_{\text{RX}_k}[j]=1,\hat{\mathbf{W}}_{\text{FC}_k}^{j-1}\right)\\&+\Pr\left(\hat{W}_{\text{RX}_k}[j]=0|W_{\text{TX}}[j],\hat{\mathbf{W}}_{\text{FC}}^{j-1}\right)\\&\times\Pr\left(S_{\text{ob},k}^{\text{FC,D}}[j]=\tilde{s}_k[j]|\hat{W}_{\text{RX}_k}[j]=0,\hat{\mathbf{W}}_{\text{FC}_k}^{j-1}\right)\Bigg]. \quad (5)\end{aligned}$$

For the evaluation of the likelihood in all future intervals, i.e., $\mathcal{L}[j+1],\ldots,\mathcal{L}[L]$, the FC also chooses the symbol $\hat{W}_{\text{FC}_k}[j]$ in the jth interval given the likelihood of the sum $\tilde{s}_k[j]$ from the RX_k-FC link in the jth interval. By doing so, $\hat{W}_{\text{FC}_k}[j]$ is obtained by

$$\hat{W}_{\text{FC}_k}[j]=\underset{\hat{W}_{\text{RX}_k}[j]\in\{0,1\}}{\text{argmax}}\ \Pr\left(S_{\text{ob},k}^{\text{FC,D}}[j]=\tilde{s}_k[j]|\hat{W}_{\text{RX}_k}[j],\hat{\mathbf{W}}_{\text{FC}_k}^{j-1}\right). \quad (6)$$

Eqs. (5) and (6) can be evaluated by applying the conditional cumulative distribution function (CDF) of the Poisson RV $S_{\text{ob}}^{\text{RX}_k}[j]$ and the conditional PMF of the Poisson RV $S_{\text{ob},k}^{\text{FC,D}}[j]$. The conditional means $\bar{S}_{\text{ob},k}^{\text{FC,D}}[j]$ given $\hat{\mathbf{W}}_{\text{FC}_k}^{j-1}$ are obtained by replacing S_0, $W_{\text{TX}}[i]$, $P_{\text{ob}}^{(\text{TX},\text{RX}_k)}$, M_{RX}, m, and Δt_{RX} in (2) with S_k, $\hat{W}_{\text{FC}_k}[i]$, $P_{\text{ob},k}^{(\text{RX}_k,\text{FC})}$, M_{FC}, $\tilde{m}$, and Δt_{FC}, respectively.

B. SD-ML

The behavior of each RX_k in SD-ML is the same as that in MD-ML, except we assume that each RX_k transmits type A_1 molecules to report $\hat{W}_{\text{RX}_k}[j]$ to the FC. This is because it may not be realistic for each RX to release a unique type of molecule. For simplicity, the number of released type A_1 molecules for each RX_k in SD-ML is also denoted by S_k. The FC receives type A_1 molecules over all K RX_k-FC links and takes M_{FC} samples of type A_1 molecules in each symbol interval. The FC adds M_{FC} observations for all RX_k-FC links in the jth symbol interval. We denote $S_{\text{ob}}^{\text{FC,D}}[j]$ as the total number of A_1 molecules observed within V_{FC} in the jth symbol interval, due to both current and previous emissions of molecules by all RXs. We note that $S_{\text{ob}}^{\text{FC,D}}[j]=\sum_{k=1}^{K}S_{\text{ob},k}^{\text{FC,D}}[j]$ is also a Poisson RV whose mean is given by $\bar{S}_{\text{ob}}^{\text{FC,D}}[j]=\sum_{k=1}^{K}\bar{S}_{\text{ob},k}^{\text{FC,D}}[j]$. Values of realizations of

$S_{\text{ob}}^{\text{FC,D}}[j]$ are labeled $\tilde{s}[j]$. The FC chooses the symbol $\hat{W}_{\text{FC}}[j]$ that is more likely, given the likelihood of $\tilde{s}[j]$ in the jth interval. To facilitate the evaluation of $\mathcal{L}[j]$ for SD-ML, we define $\hat{\mathcal{W}}_l^{\text{FC}} = \{\hat{W}_{\text{FC}_1}[l], \ldots, \hat{W}_{\text{FC}_K}[l]\}$. Using the notation $\hat{\mathcal{W}}_l^{\text{FC}}$, we derive $\mathcal{L}[j]$ as

$$\mathcal{L}[j] = \sum_{h=1}^{2^K} \Big[\Pr\left(\hat{\mathcal{W}}_{j,h}^{\text{RX}} | W_{\text{TX}}[j], \hat{\mathbf{W}}_{\text{FC}}^{j-1}\right) \times \Pr\left(S_{\text{ob}}^{\text{FC,D}}[j] = \tilde{s}[j] | \hat{\mathcal{W}}_{j,h}^{\text{RX}}, \hat{\mathcal{W}}_{j-1}^{\text{FC}}, \ldots, \hat{\mathcal{W}}_1^{\text{FC}}\right)\Big], \quad (7)$$

where $\hat{\mathcal{W}}_{j,h}^{\text{RX}}$ is the hth realization of the vector $\{\hat{W}_{\text{RX}_1}[j], \ldots, \hat{W}_{\text{RX}_K}[j]\}$, $h \in \{1, 2, \ldots, 2^K\}$. For (7), we need to consider each $\hat{\mathcal{W}}_{j,h}^{\text{RX}}$ and the corresponding probability leading to $\tilde{s}[j]$. For the evaluation of the likelihood in all future intervals, the FC chooses $\hat{\mathcal{W}}_j^{\text{FC}}$ that gives the maximum likelihood of $\tilde{s}[j]$. By doing so, $\hat{\mathcal{W}}_j^{\text{FC}}$ is obtained by

$$\hat{\mathcal{W}}_j^{\text{FC}} = \underset{\hat{\mathcal{W}}_{j,h}^{\text{RX}}}{\text{argmax}} \Pr\Big(S_{\text{ob}}^{\text{FC,D}}[j] = \tilde{s}[j] | \hat{\mathcal{W}}_{j,h}^{\text{RX}}, \hat{\mathcal{W}}_{j-1}^{\text{FC}}, \ldots, \hat{\mathcal{W}}_1^{\text{FC}}\Big). \quad (8)$$

We now derive the conditional mean of $S_{\text{ob}}^{\text{FC,D}}[j]$ given $\hat{\mathcal{W}}_{j,h}^{\text{RX}}$ and $\hat{\mathcal{W}}_{j-1}^{\text{FC}}, \ldots, \hat{\mathcal{W}}_1^{\text{FC}}$. To this end, we evaluate $\bar{S}_{\text{ob}}^{\text{FC,D}}[j]$ as

$$\bar{S}_{\text{ob}}^{\text{FC,D}}[j] = \sum_{k=1}^{K} \sum_{\tilde{m}=1}^{M_{\text{FC}}} S_k \Big(\hat{W}_{\text{RX}_k}[j] P_{\text{ob},k}^{(\text{RX}_k,\text{FC})}(\tilde{m}\Delta t_{\text{FC}}) + \sum_{i=1}^{j-1} \hat{W}_{\text{FC}_k}[i] P_{\text{ob},k}^{(\text{RX}_k,\text{FC})}((j-i)T + \tilde{m}\Delta t_{\text{FC}}) \Big). \quad (9)$$

C. SA-ML

For SA-ML, each RX amplifies the number of molecules observed in the jth symbol interval, i.e., $S_k^{\text{A}}[j] = \alpha_k S_{\text{ob}}^{\text{RX}_k}[j]$, where $S_k^{\text{A}}[j]$ denotes the number of molecules released by RX_k in the jth symbol interval and α_k is the *constant* amplification factor at RX_k. The RXs retransmit $S_k^{\text{A}}[j]$ molecules of type A_1 to the FC at the same time. Since all RXs in both SA-ML and SD-ML release molecules of the same type A_1, the description of the behavior of the FC in SA-ML is analogous to that in SD-ML. We denote $S_{\text{ob},k}^{\text{FC,A}}[j]$ as the number of molecules observed within V_{FC} in the jth symbol interval, due to the emissions of molecules from the current and the previous intervals by RX_k. The $\text{TX} - \text{RX}_k$ and $\text{RX}_k - \text{FC}$ links are both diffusion-based. Therefore, $S_{\text{ob},k}^{\text{FC,A}}[j]$ can be accurately approximated as a Poisson RV. We denote $\bar{S}_{\text{ob},k}^{\text{FC,A}}[j]$ as the mean of $S_{\text{ob},k}^{\text{FC,A}}[j]$. The FC adds M_{FC} observations for all $\text{RX}_k - \text{FC}$ links in the jth symbol interval and this sum is denoted by the RV $S_{\text{ob}}^{\text{FC,A}}[j]$. We note that $S_{\text{ob}}^{\text{FC,A}}[j] = \sum_{k=1}^{K} S_{\text{ob},k}^{\text{FC,A}}[j]$ is also a Poisson RV whose mean is given by $\bar{S}_{\text{ob}}^{\text{FC,A}}[j] = \sum_{k=1}^{K} \bar{S}_{\text{ob},k}^{\text{FC,A}}[j]$. Values of realizations of $S_{\text{ob}}^{\text{FC,A}}[j]$ are labeled $\tilde{s}[j]$. The FC chooses the symbol $\hat{W}_{\text{FC}}[j]$ that is more likely given the likelihood of $\tilde{s}[j]$ in the jth interval and $\mathcal{L}[j]$ is given in (10) at the top of the following page. where $S_{\text{ob}}^{\text{RX}_k}[i]$ and $s_k[i]$, $i \in \{1, \ldots, j\}$ and $k \in \{1, \ldots, K\}$, are defined in Section II-A.

Theoretically, any number of molecules between 0 and S_0 can be observed at each RX. Thus, there is a large number of realizations for each Poisson RV $S_{\text{ob}}^{\text{RX}_k}[i]$ in (10), which makes the complete evaluation of (10) cumbersome. To simplify the evaluation of (10), we consider finitely many random realizations of each Poisson RV $S_{\text{ob}}^{\text{RX}_k}[i]$[4]. For example, we generate 5000 random realizations of each $S_{\text{ob}}^{\text{RX}_k}[i]$ for a given $\hat{\mathbf{W}}_{\text{FC}}^{j-1}$, which is sufficient to ensure the accuracy of (10). It is shown that (10) can be evaluated by applying the conditional PMF of the Poisson RV $S_{\text{ob}}^{\text{FC,A}}[j]$. We obtain the conditional mean of $S_{\text{ob},k}^{\text{FC,A}}[j]$ by replacing $S_0 W_{\text{TX}}[i]$, $P_{\text{ob}}^{(\text{TX},\text{RX}_k)}$, M_{RX}, m, and Δt_{RX} in (2) with $S_k^{\text{A}}[j]$, $P_{\text{ob},k}^{(\text{RX}_k,\text{FC})}$, M_{FC}, $\tilde{m}$, and Δt_{FC}, respectively. Based on $\bar{S}_{\text{ob}}^{\text{FC,A}}[j] = \sum_{k=1}^{K} \bar{S}_{\text{ob},k}^{\text{FC,A}}[j]$, we can then obtain the conditional mean of $S_{\text{ob}}^{\text{FC,A}}[j]$.

D. Comparison of Complexity

We summarize the complexity comparison in Table I. MD-ML requires higher complexity than SD-ML. This is because each RX releases a unique type of molecule in MD-ML, whereas in SD-ML the RXs release a single type of molecule. SD-ML requires higher complexity than SA-ML. This is because the RXs need to decode the TX's symbols and the FC needs to estimate the RXs' decisions in SD-ML, but in SA-ML the RXs only need to amplify the received signal and the FC does not need to estimate the RXs' decisions.

IV. Error Performance Analysis

In this section, we derive the error probability of SD-ML and SA-ML using the *genie-aided history*, which leads to tractable expressions. Also, the error probability with genie-aided history provides a lower bound on that with local history. We denote $Q_{\text{FC}}[j]$ as the error probability of the system in the jth symbol interval for a TX sequence $\mathbf{W}_{\text{TX}}^{j-1}$. The closed-form expressions of $Q_{\text{FC}}[j]$ for SD-ML with $K = 1$ and SA-ML are mathematically tractable.

To derive $Q_{\text{FC}}[j]$, we first derive equivalent decision rules with lower-complexity than (3) and (4) for SD-ML and SA-ML in Theorems 1 and 2, respectively. The decision rules when not all previously-transmitted symbols are "0" cannot be directly applied to the case where all previously-transmitted symbols are "0". Based on these theorems, the general forms of these lower-complexity decision rules are that the FC compares the observation with *adaptive* thresholds when not all previously-transmitted symbols are "0" and the FC compares the observation with 0 when all previously-transmitted symbols are "0". Notably, these adaptive thresholds adapt to different ISI in different symbol intervals.

A. SD-ML

We now derive $Q_{\text{FC}}[j]$ for the SD-ML variant. To this end, we first define $\hat{\lambda}_1^{\text{D}}[j]$ as the expected ISI at the FC in the jth symbol interval due to the previous symbols transmitted by all RXs, $\hat{\mathbf{W}}_{\text{RX}_1}^{j-1}, \hat{\mathbf{W}}_{\text{RX}_2}^{j-1}, \ldots, \hat{\mathbf{W}}_{\text{RX}_K}^{j-1}$, i.e.,

$$\hat{\lambda}_1^{\text{D}}[j] = \sum_{k=1}^{K} S_k \sum_{i=1}^{j-1} \hat{W}_{\text{RX}_k}[i] \sum_{\tilde{m}=1}^{M_{\text{FC}}} P_{\text{ob},k}^{(\text{RX}_k,\text{FC})}((j-i)T + \tilde{m}\Delta t_{\text{FC}}). \quad (11)$$

[4]We assume that the FC may have sufficiently high computational capabilities such that it can generate random realizations. This assumption is because the FC could have a direct interface to additional computational resources.

$$\mathcal{L}[j] = \sum_{s_1[1]=0}^{S_0} \cdots \sum_{s_1[j]=0}^{S_0} \cdots \sum_{s_K[1]=0}^{S_0} \cdots \sum_{s_K[j]=0}^{S_0} \times \Pr\Big(S_{\text{ob}}^{\text{RX}_1}[1] = s_1[1], \ldots, S_{\text{ob}}^{\text{RX}_1}[j] = s_1[j], \ldots, S_{\text{ob}}^{\text{RX}_K}[1] = s_K[1], \ldots, S_{\text{ob}}^{\text{RX}_K}[j] = s_K[j] | W_{\text{TX}}[j], \hat{\mathbf{W}}_{\text{FC}}^{j-1}\Big) \times \Pr\Big(S_{\text{ob}}^{\text{FC,A}}[j] = \tilde{s}[j] | S_{\text{ob}}^{\text{RX}_1}[1] = s_1[1], \ldots, S_{\text{ob}}^{\text{RX}_1}[j] = s_1[j], \ldots, S_{\text{ob}}^{\text{RX}_K}[1] = s_K[1], \ldots, S_{\text{ob}}^{\text{RX}_K}[j] = s_K[j]\Big), \quad (10)$$

If not all previous symbols transmitted by all RXs are "0". i.e., $\sum_{i=1}^{j-1}\sum_{k=1}^{K} \hat{W}_{\text{RX}_k}[i] \neq 0$, we have $\hat{\lambda}_{\text{I}}^{\text{D}}[j] > 0$; otherwise, we have $\hat{\lambda}_{\text{I}}^{\text{D}}[j] = 0$. We then define $\hat{\lambda}_{\text{s},h}^{\text{D,tot}}[j]$ as the total number of signal molecules at the FC in the jth symbol interval due to the hth realization of currently-transmitted RX symbols $\hat{\mathcal{W}}_{j,h}^{\text{RX}}$, i.e.,

$$\hat{\lambda}_{\text{s},h}^{\text{D,tot}}[j] = \sum_{k=1}^{K} S_k \hat{W}_{\text{RX}_k}[j] \sum_{\tilde{m}=1}^{M_{\text{FC}}} P_{\text{ob},k}^{(\text{RX}_k,\text{FC})}(\tilde{m}\Delta t_{\text{FC}}). \quad (12)$$

For the sake of brevity, for SD-ML, we define $\mathcal{L}\left[j|W_{\text{TX}}[j]=1, \mathbf{W}_{\text{TX}}^{j-1}, \hat{\mathbf{W}}_{\text{RX}_k}^{j-1}\right] \triangleq \mathcal{L}_1^{\text{SD}}[j]$ and $\mathcal{L}\left[j|W_{\text{TX}}[j]=0, \mathbf{W}_{\text{TX}}^{j-1}, \hat{\mathbf{W}}_{\text{RX}_k}^{j-1}\right] \triangleq \mathcal{L}_0^{\text{SD}}[j]$. Applying the conditional PMF of $S_{\text{ob}}^{\text{FC,D}}[j]$ to (7), we write $\mathcal{L}_b^{\text{SD}}[j]$ as

$$\mathcal{L}_b^{\text{SD}}[j] = \sum_{h=1}^{2^K} \Bigg[\Pr\left(\hat{\mathcal{W}}_{j,h}^{\text{RX}} | W_{\text{TX}}[j]=b, \mathbf{W}_{\text{TX}}^{j-1}\right)(\tilde{s}[j]!)^{-1} \times \exp\Big(-\hat{\lambda}_{\text{I}}^{\text{D}}[j] - \hat{\lambda}_{\text{s},h}^{\text{D,tot}}[j]\Big)\left(\hat{\lambda}_{\text{I}}^{\text{D}}[j] + \hat{\lambda}_{\text{s},h}^{\text{D,tot}}[j]\right)^{\tilde{s}[j]}\Bigg], \quad (13)$$

where $b \in \{0,1\}$. Based on (13), we rederive the decision rule of SD-ML in (4) as a lower-complexity decision rule in the following theorem.

Theorem 1: When $\hat{\lambda}_{\text{I}}^{\text{D}}[j] > 0$, the decision rule of SD-ML is $\hat{W}_{\text{FC}}[j] = 1$ if $\tilde{s}[j] \geq \xi_{\text{FC}}^{\text{ad,SD}}[j]$; otherwise, $\hat{W}_{\text{FC}}[j] = 0$, where $\xi_{\text{FC}}^{\text{ad,SD}}[j]$ is the solution to $\mathcal{L}_1^{\text{SD}}[j] = \mathcal{L}_0^{\text{SD}}[j]$ in terms of $\tilde{s}[j]$. We note that $\mathcal{L}_1^{\text{SD}}[j] = \mathcal{L}_0^{\text{SD}}[j]$ has a solution only when $\hat{\lambda}_{\text{I}}^{\text{D}}[j] > 0$. When $\hat{\lambda}_{\text{I}}^{\text{D}}[j] = 0$, the decision rule for SD-ML is $\hat{W}_{\text{FC}}[j] = 1$ if $\tilde{s}[j] > 0$ and $\hat{W}_{\text{FC}}[j] = 0$ if $\tilde{s}[j] = 0$,

Proof: Please see Appendix A. ∎

Based on Theorem 1, when $\hat{\lambda}_{\text{I}}^{\text{D}}[j] > 0$, we evaluate the conditional Q_{FC} as

$$Q_{\text{FC}}\left[j|\hat{\lambda}_{\text{I}}^{\text{D}}[j] > 0\right] = P_1 \Pr\left(S_{\text{ob}}^{\text{FC,D}}[j] < \xi_{\text{FC}}^{\text{ad,SD}}[j] | W_{\text{TX}}[j]=1, \hat{\lambda}_{\text{I}}^{\text{D}}[j] > 0\right) + (1-P_1)\Pr\left(S_{\text{ob}}^{\text{FC,D}}[j] \geq \xi_{\text{FC}}^{\text{ad,SD}}[j] | W_{\text{TX}}[j]=0, \hat{\lambda}_{\text{I}}^{\text{D}}[j] > 0\right), \quad (14)$$

where the conditional CDF of the Poisson RV $S_{\text{ob}}^{\text{FC,D}}[j]$ can be evaluated by

$$\Pr\left(S_{\text{ob}}^{\text{FC,D}}[j] < \xi_{\text{FC}}^{\text{ad,SD}}[j] | W_{\text{TX}}[j], \hat{\lambda}_{\text{I}}^{\text{D}}[j]\right) = \sum_{h=1}^{2^K}\Bigg[\Pr\left(\hat{\mathcal{W}}_{j,h}^{\text{RX}} | W_{\text{TX}}[j], \mathbf{W}_{\text{TX}}^{j-1}\right)\exp\left(-\hat{\lambda}_{\text{I}}^{\text{D}}[j] - \hat{\lambda}_{\text{s},h}^{\text{D,tot}}[j]\right) \times \sum_{\eta=0}^{\xi_{\text{FC}}^{\text{ad,SD}}[j]-1}\left(\hat{\lambda}_{\text{I}}^{\text{D}}[j] + \hat{\lambda}_{\text{s},h}^{\text{D,tot}}[j]\right)^{\eta}/(\eta!)\Bigg], \quad (15)$$

where $\hat{\lambda}_{\text{I}}^{\text{D}}[j]$ can be evaluated by (11) via the approximated $\hat{\mathbf{W}}_{\text{RX}_k}^{j-1}$, $k \in \{1,2,\ldots,K\}$. The approximated $\hat{\mathbf{W}}_{\text{RX}_k}^{j-1}$ can be obtained using the biased coin toss method introduced in [31]. Specifically, we model the ith decision at RX_k, $\hat{W}_{\text{RX}_k}[i]$, as $\hat{W}_{\text{RX}_k}[i] = |\lambda - W_{\text{TX}}[i]|$, where $i \in \{1,\ldots,j-1\}$ and $\lambda \in \{0,1\}$ is the outcome of the coin toss with $\Pr(\lambda=1) = \Pr\left(\hat{W}_{\text{RX}_k}[i]=0 | W_{\text{TX}}[i]=1\right)$ if $W_{\text{TX}}[i]=1$ and $\Pr(\lambda=1) = \Pr\left(\hat{W}_{\text{RX}_k}[i]=1 | W_{\text{TX}}[i]=0\right)$ if $W_{\text{TX}}[i]=0$. When $\hat{\lambda}_{\text{I}}^{\text{D}}[j]=0$, we evaluate the conditional Q_{FC} as

$$Q_{\text{FC}}\left[j|\hat{\lambda}_{\text{I}}^{\text{D}}[j]=0\right] = P_1 \Pr\left(S_{\text{ob}}^{\text{FC,D}}[j]=0 | W_{\text{TX}}[j]=1, \hat{\lambda}_{\text{I}}^{\text{D}}[j]=0\right) + (1-P_1)\Pr\left(S_{\text{ob}}^{\text{FC,D}}[j]>0 | W_{\text{TX}}[j]=0, \hat{\lambda}_{\text{I}}^{\text{D}}[j]=0\right), \quad (16)$$

where the conditional CDF of the Poisson RV $S_{\text{ob}}^{\text{FC,D}}[j]$ can be evaluated analogously to (15). Combining (16) and (14), we obtain $Q_{\text{FC}}[j]$ for SD-ML as

$$Q_{\text{FC}}[j] = \Pr\left(\hat{\lambda}_{\text{I}}^{\text{D}}[j] > 0 | \mathbf{W}_{\text{TX}}^{j-1}\right) Q_{\text{FC}}\left[j|\hat{\lambda}_{\text{I}}^{\text{D}}[j] > 0\right] + \Pr\left(\hat{\lambda}_{\text{I}}^{\text{D}}[j]=0 | \mathbf{W}_{\text{TX}}^{j-1}\right) Q_{\text{FC}}\left[j|\hat{\lambda}_{\text{I}}^{\text{D}}[j]=0\right]. \quad (17)$$

Finally, we derive the closed-form expression for $Q_{\text{FC}}[j]$ for SD-ML with $K=1$. To this end, we first rewrite $\mathcal{L}_1^{\text{SD}}[j]$ and $\mathcal{L}_0^{\text{SD}}[j]$ using (13) with $K=1$. We then solve $\mathcal{L}_1^{\text{SD}}[j] = \mathcal{L}_0^{\text{SD}}[j]$ in terms of $\xi_{\text{FC}}^{\text{ad,SD}}[j]$ and obtain the closed-form expression for $\xi_{\text{FC}}^{\text{ad,SD}}[j]$ when $K=1$ as $\xi_{\text{FC}}^{\text{ad,SD}}[j] = \left\lfloor \hat{\lambda}_{\text{s}}^{\text{D}}[j] / \log\left(\hat{\lambda}_{\text{I}}^{\text{D}}[j] + \hat{\lambda}_{\text{s}}^{\text{D}}[j]/\hat{\lambda}_{\text{I}}^{\text{D}}[j]\right)\right\rfloor$. We note that $Q_{\text{FC}}[j]$ for SD-ML with $K=1$ can be obtained using (17) via this expression.

B. SA-ML

We now derive $Q_{\text{FC}}[j]$ for SA-ML. In (10), multiple possible realizations of each Poisson RV $S_{\text{ob}}^{\text{RX}_k}[i]$ make the analytical error performance analysis cumbersome. To facilitate the error performance analysis, we consider only one random realization

of $S_{\text{ob}}^{\text{RX}_k}[i]$ with the mean $\bar{S}_{\text{ob}}^{\text{RX}_k}[i]$ for the *given* previous symbols transmitted by the TX, $\mathbf{W}_{\text{TX}}^{j-1}$. We define $\hat{\lambda}_{\text{I}}^{\text{A}}[j]$ as the expected ISI at the FC in the jth symbol interval due to $\mathbf{W}_{\text{TX}}^{j-1}$. We define $\hat{\lambda}_{\text{S}}^{\text{A}}[j]$ as the number of the signal molecules at the FC in the jth symbol interval due to $W_{\text{TX}}[j]=1$. By modeling the realization of $S_{\text{ob}}^{\text{RX}_k}[i]$ as its mean $\bar{S}_{\text{ob}}^{\text{RX}_k}[i]$, we write $\hat{\lambda}_{\text{I}}^{\text{A}}[j]$ and $\hat{\lambda}_{\text{S}}^{\text{A}}[j]$ as

$$\hat{\lambda}_{\text{I}}^{\text{A}}[j]=\sum_{k=1}^{K}\Bigg(\sum_{i=1}^{j-1}\alpha_k\bar{S}_{\text{ob}}^{\text{RX}_k}[i]\sum_{\tilde{m}=1}^{M_{\text{FC}}}P_{\text{ob},k}^{(\text{RX}_k,\text{FC})}\left((j-i)\,T+\tilde{m}\Delta t_{\text{FC}}\right)+\alpha_k S_0\sum_{i=1}^{j-1}W_{\text{TX}}[i]\sum_{m=1}^{M_{\text{RX}}}P_{\text{ob}}^{(\text{TX},\text{RX})}((j-i)T+m\Delta t_{\text{RX}})\times\sum_{\tilde{m}=1}^{M_{\text{FC}}}P_{\text{ob},k}^{(\text{RX}_k,\text{FC})}\left(\tilde{m}\Delta t_{\text{FC}}\right)\Bigg) \tag{18}$$

and

$$\hat{\lambda}_{\text{S}}^{\text{A}}[j]=\sum_{k=1}^{K}\alpha_k S_0\sum_{m=1}^{M_{\text{RX}}}P_{\text{ob}}^{(\text{TX},\text{RX})}(m\Delta t_{\text{RX}})\sum_{\tilde{m}=1}^{M_{\text{FC}}}P_{\text{ob},k}^{(\text{RX}_k,\text{FC})}\left(\tilde{m}\Delta t_{\text{FC}}\right), \tag{19}$$

respectively. $\hat{\lambda}_{\text{I}}^{\text{A}}[j]$ in (18) consists of two components. The first summation over i is the expected ISI at the FC in the jth symbol interval due to the molecules released by the RXs but without the amplification of the RXs' ISI from the TX. The second summation over i accounts for the amplification of the ISI in the jth symbol interval at all RXs due to $\mathbf{W}_{\text{TX}}^{j-1}$. We note that the conditional mean of $S_{\text{ob}}^{\text{FC,A}}[j]$ is $\hat{\lambda}_{\text{S}}^{\text{A}}[j]+\hat{\lambda}_{\text{I}}^{\text{A}}[j]$ when $W_{\text{TX}}[j]=1$, and the conditional mean of $S_{\text{ob}}^{\text{FC,A}}[j]$ is $\hat{\lambda}_{\text{I}}^{\text{A}}[j]$ when $W_{\text{TX}}[j]=0$. If not all previous symbols transmitted by the TX are "0". i.e., $\mathbf{W}_{\text{TX}}^{j-1}\neq\mathbf{0}$, then we have $\hat{\lambda}_{\text{I}}^{\text{A}}[j]>0$. If all previous symbols transmitted by the TX are "0", i.e., $\mathbf{W}_{\text{TX}}^{j-1}=\mathbf{0}$, then we have $\hat{\lambda}_{\text{I}}^{\text{A}}[j]=0$. For the sake of brevity, for SA-ML, we define $\mathcal{L}\left[j|W_{\text{TX}}[j]=1,\mathbf{W}_{\text{TX}}^{j-1}\right]\triangleq\mathcal{L}_1^{\text{SA}}$ and $\mathcal{L}\left[j|W_{\text{TX}}[j]=0,\mathbf{W}_{\text{TX}}^{j-1}\right]\triangleq\mathcal{L}_0^{\text{SA}}$. Applying the conditional PMF of the Poisson RV $S_{\text{ob}}^{\text{FC,A}}[j]$ to (10), we derive $\mathcal{L}_1^{\text{SA}}$ and $\mathcal{L}_0^{\text{SA}}$ as

$$\mathcal{L}_1^{\text{SA}}=\frac{\left(\hat{\lambda}_{\text{S}}^{\text{A}}[j]+\hat{\lambda}_{\text{I}}^{\text{A}}[j]\right)^{\tilde{s}[j]}\exp\left(-\left(\hat{\lambda}_{\text{S}}^{\text{A}}[j]+\hat{\lambda}_{\text{I}}^{\text{A}}[j]\right)\right)}{\tilde{s}[j]!} \tag{20}$$

and

$$\mathcal{L}_0^{\text{SA}}=\frac{\left(\hat{\lambda}_{\text{I}}^{\text{A}}[j]\right)^{\tilde{s}[j]}\exp\left(-\hat{\lambda}_{\text{I}}^{\text{A}}[j]\right)}{(\tilde{s}[j]!)}, \tag{21}$$

respectively. Based on (20) and (21), we rewrite the general decision rule of SA-ML in (3) as a lower-complexity decision rule in the following theorem.

Theorem 2: When $\hat{\lambda}_{\text{I}}^{\text{A}}[j]>0$, the decision rule of SA-ML is $\hat{W}_{\text{FC}}[j]=1$ if $\tilde{s}[j]\geq\xi_{\text{FC}}^{\text{ad,SA}}[j]$; otherwise, $\hat{W}_{\text{FC}}[j]=0$, where $\xi_{\text{FC}}^{\text{ad,SA}}[j]=\left\lfloor\hat{\lambda}_{\text{S}}^{\text{A}}[j]/\log\left(\hat{\lambda}_{\text{I}}^{\text{A}}[j]+\hat{\lambda}_{\text{S}}^{\text{A}}[j]/\hat{\lambda}_{\text{I}}^{\text{A}}[j]\right)\right\rfloor$. When $\hat{\lambda}_{\text{I}}^{\text{A}}[j]=0$, the decision rule is $\hat{W}_{\text{FC}}[j]=1$ if $\tilde{s}[j]>0$ and $\hat{W}_{\text{FC}}[j]=0$ if $\tilde{s}[j]=0$.

Proof: The proof is omitted here due to limited space; please refer to our arXiv version. It can be proven by applying (20) and (21) to (3) and using basic manipulations. ■

Based on Theorem 2, when $\mathbf{W}_{\text{TX}}^{j-1}\neq\mathbf{0}$, we evaluate $Q_{\text{FC}}[j]$ for SA-ML as

$$\begin{aligned}Q_{\text{FC}}[j]=&\,(1-P_1)\Pr\left(S_{\text{ob}}^{\text{FC,A}}[j]\geq\xi_{\text{FC}}^{\text{ad,SA}}[j]|W_{\text{TX}}[j]=0,\mathbf{W}_{\text{TX}}^{j-1}\right)\\&+P_1\Pr\left(S_{\text{ob}}^{\text{FC,A}}[j]<\xi_{\text{FC}}^{\text{ad,SA}}[j]|W_{\text{TX}}[j]=1,\mathbf{W}_{\text{TX}}^{j-1}\right),\end{aligned} \tag{22}$$

where $\Pr\left(S_{\text{ob}}^{\text{FC,A}}[j]<\xi_{\text{FC}}^{\text{ad,SA}}[j]|\mathbf{W}_{\text{TX}}^{j}\right)$ can be evaluated by replacing $\hat{\mathbf{W}}_{\text{FC}}^{j-1}$ and $S_{\text{ob}}^{\text{FC,A}}[j]=\tilde{s}[j]$ in (10) with $\mathbf{W}_{\text{TX}}^{j-1}$ and $S_{\text{ob}}^{\text{FC,A}}[j]<\xi_{\text{FC}}^{\text{ad,SA}}[j]$, respectively. Similar to the evaluation of (10), we consider finitely many random realizations of $S_{\text{ob}}^{\text{RX}_k}[i]$ in (22). When $\mathbf{W}_{\text{TX}}^{j-1}=\mathbf{0}$, $Q_{\text{FC}}[j]$ for SA-ML can be obtained by replacing $\geq$, $<$, and $\xi_{\text{FC}}^{\text{ad,SA}}[j]$ with $>$, $=$, and 0 in (22), respectively.

V. Error Performance Optimization

In this section, we determine the optimal molecule distribution among RXs that minimizes the error probability of SD-ML using the genie-aided history, inspired by the fact the quantity of any type of molecule is usually constrained in practical biological environments. We also analytically prove that the equal allocation of molecules among two symmetric RXs achieves the local minimal error probability of SD-ML.

To this end, we first formulate the optimization problem as follows:

$$\begin{aligned}\min_{\mathbf{S}}\quad&Q_{\text{FC}}[j]\text{ in (17)}\\\text{s.t.}\quad&S_1+S_2+\cdots+S_K-N=0,\\&S_k\geq 0,\end{aligned} \tag{23}$$

where $\mathbf{S}=\{S_1,S_2,\ldots,S_K\}$, $k\in\{1,2,\ldots,K\}$, and N is the total number of molecules released by K RXs for symbol "1". Combining (14) and (17), we note that $\xi_{\text{FC}}^{\text{ad,SD}}[j]$ is required to evaluate $Q_{\text{FC}}[j]$. Based on Theorem 1, the adaptive threshold $\xi_{\text{FC}}^{\text{ad,SD}}[j]$ is obtained by numerically solving $\mathcal{L}_1^{\text{SD}}[j]=\mathcal{L}_0^{\text{SD}}[j]$ in terms of $\tilde{s}[j]$, while the closed-form expression for $\xi_{\text{FC}}^{\text{ad,SD}}[j]$ is mathematically intractable. Therefore, there is no closed-form expression for $Q_{\text{FC}}[j]$, which makes it very hard to optimize $Q_{\text{FC}}[j]$ in (17). To tackle this challenge, we find a closed-form approximation for $Q_{\text{FC}}[j]$ in (17) by considering a constant threshold ξ in (14). By doing so, we find the approximation of $Q_{\text{FC}}[j]$ as

$$\begin{aligned}Q_{\text{FC}}^{\sharp}[j]=&\,P_1\sum_{h=1}^{2^K}\left[\Pr\left(\hat{\mathcal{W}}_{j,h}^{\text{RX}}|W_{\text{TX}}[j]=1,\mathbf{W}_{\text{TX}}^{j-1}\right)\Lambda\right]\\&+(1-P_1)\sum_{h=1}^{2^K}\left[\Pr\left(\hat{\mathcal{W}}_{j,h}^{\text{RX}}|W_{\text{TX}}[j]=0,\mathbf{W}_{\text{TX}}^{j-1}\right)\times(1-\Lambda)\right],\end{aligned} \tag{24}$$

where $Q_{\text{FC}}^{\sharp}[j]$ is the approximation of $Q_{\text{FC}}[j]$, Λ is given by

$$\Lambda=\sum_{\eta=0}^{\xi-1}\exp\left(-\hat{\lambda}_{\text{I}}^{\text{D}}[j]-\hat{\lambda}_{\text{S},h}^{\text{D,tot}}[j]\right)\frac{\left(\hat{\lambda}_{\text{I}}^{\text{D}}[j]+\hat{\lambda}_{\text{S},h}^{\text{D,tot}}[j]\right)^{\eta}}{(\eta!)}, \tag{25}$$

and ξ is a constant. In (25), $\hat{\lambda}_{\text{I}}^{\text{D}}[j]$ and $\hat{\lambda}_{\text{S},h}^{\text{D,tot}}[j]$ are the functions of $\mathbf{S}$ based on (11) and (12).

Lemma 1: The approximation of $Q_{\text{FC}}[j]$ by $Q^{\sharp}_{\text{FC}}[j]$ is tight when $\xi = \xi^{\text{ad,SD}}_{\text{FC}}[j]$.

Proof: We note that the likelihood of the occurrence that all previous symbols transmitted by all RXs are "0" is very small. Thus, we approximate $\Pr\left(\hat{\lambda}^{\text{D}}_{\text{I}}[j]=0|\mathbf{W}^{j-1}_{\text{TX}}\right) \approx 0$ and $\Pr\left(\hat{\lambda}^{\text{D}}_{\text{I}}[j]>0|\mathbf{W}^{j-1}_{\text{TX}}\right) \approx 1$. Using these approximations in (17), we obtain $Q_{\text{FC}}[j] \approx Q_{\text{FC}}\left[j|\hat{\lambda}^{\text{D}}_{\text{I}}[j]>0\right]$. We then note that $Q^{\sharp}_{\text{FC}}[j]|_{\xi=\xi^{\text{ad,SD}}_{\text{FC}}[j]} = Q_{\text{FC}}\left[j|\hat{\lambda}^{\text{D}}_{\text{I}}[j]>0\right]$. Thus, $Q_{\text{FC}}[j]$ is accurately approximated by $Q^{\sharp}_{\text{FC}}[j]$ when $\xi = \xi^{\text{ad,SD}}_{\text{FC}}[j]$. ∎

Lemma 2: Since the adaptive threshold $\xi^{\text{ad,SD}}_{\text{FC}}[j]$ adapts to different ISI for different symbol intervals, $\xi^{\text{ad,SD}}_{\text{FC}}[j]$ is the optimal ξ that minimizes $Q^{\sharp}_{\text{FC}}[j]$ if $P_1 = \frac{1}{2}$, i.e., $\xi^{\text{ad,SD}}_{\text{FC}}[j] = \underset{\xi}{\text{argmin}}\, Q^{\sharp}_{\text{FC}}[j]$.

Proof: Please see Appendix B. ∎

Based on Lemma 1 and Lemma 2, the approximation of $Q_{\text{FC}}[j]$ by $Q^{\sharp}_{\text{FC}}[j]$ is tight when $\xi = \xi^{\text{ad,SD}}_{\text{FC}}[j]$ and $\xi^{\text{ad,SD}}_{\text{FC}}[j]$ is the optimal ξ which minimizes $Q^{\sharp}_{\text{FC}}[j]$. Therefore, the optimal $\mathbf{S}$ that minimizes $Q_{\text{FC}}[j]$ in (17) can be obtained by finding the jointly optimal $\mathbf{S}$ and ξ to minimize $Q^{\sharp}_{\text{FC}}[j]$ in (24), i.e., the approximate solution to the problem (23) can be obtained by solving the optimization problem given by:

$$\begin{aligned} \min_{\mathbf{S},\,\xi} \quad & Q^{\sharp}_{\text{FC}}[j] \\ \text{s.t.} \quad & S_1 + S_2 + \cdots + S_K - N = 0, \\ & S_k \geq 0. \end{aligned} \tag{26}$$

To solve (26), we examine its convexity. The convexity of an optimization problem can be proven by showing that its objective function and constraints are convex with respect to the optimization variables. Since the constraints in (26) are affine, they are convex. The convexity of the objective function, i.e., $Q^{\sharp}_{\text{FC}}[j]$, can be proven by showing that its Hessian is positive semidefinite with respect to its optimization variables. For the convexity of $Q^{\sharp}_{\text{FC}}[j]$, we have the following proposition:

Proposition 1: The Hessian of $Q^{\sharp}_{\text{FC}}[j]$ is not positive semidefinite with respect to $\mathbf{S}$ and ξ.

Proof: Please see Appendix C. ∎

Based on Proposition 1, the multi-dimensional optimization problem (26) is not a convex optimization problem. To overcome this challenge, we use GlobalSearch in MATLAB to repeatedly run a local solver with the sequential quadratic programming (SQP) algorithm until convergence is achieved (i.e., the global minimum is found) to solve the problem (26). Our numerical results in Section VI confirm the effectiveness of this optimization method.

To obtain additional analytical insights in molecule distribution, we discuss the optimal distribution of the number of molecules in a symmetric topology. Intuitively, we expect that an equal distribution of molecules among symmetric RXs is the optimal allocation to minimize the error probability. To confirm this conjecture, we first find that the equal distribution locally minimizes $Q^{\sharp}_{\text{FC}}[j]$ under certain conditions. We derive such conditions in the following Lemma:

Lemma 3: In the symmetric topology with $K = 2$, if $\Upsilon(\xi) > 0$, $Q^{\sharp}_{\text{FC}}[j]$ achieves a local minimum when $S_1 = \frac{N}{2}$; otherwise, it achieves a local maximum, where $\Upsilon(\xi)$ is given by

$$\Upsilon(\xi) = \left(\alpha(P_1-1) + \beta P_1\right)\left(2 + N(\nu+2\sigma) - 2\lceil\xi\rceil\right), \tag{27}$$

where

$$\begin{aligned} &\sigma_1 = \sigma_2 = \sigma,\ \nu_1 = \nu_2 = \nu, \\ &\alpha(1,0) = \alpha(0,1) = \alpha,\ \text{and}\ \beta(1,0) = \beta(0,1) = \beta, \end{aligned} \tag{28}$$

$$\sigma_k = \sum_{i=1}^{j-1} \hat{W}_{\text{RX}_k}[i] \sum_{\tilde{m}=1}^{M_{\text{FC}}} P^{(\text{RX}_k,\text{FC})}_{\text{ob},k}\left((j-i)\,T + \tilde{m}\Delta t_{\text{FC}}\right), \tag{29}$$

$$\nu_k = \sum_{\tilde{m}=1}^{M_{\text{FC}}} P^{(\text{RX}_k,\text{FC})}_{\text{ob},k}\left(\tilde{m}\Delta t_{\text{FC}}\right), \tag{30}$$

$$\begin{aligned} \alpha(a_1,a_2) = &\Pr\left(\hat{W}_{\text{RX}_1}[j]=a_1|W_{\text{TX}}[j]=0,\mathbf{W}^{j-1}_{\text{TX}}\right) \\ &\times \Pr\left(\hat{W}_{\text{RX}_2}[j]=a_2|W_{\text{TX}}[j]=0,\mathbf{W}^{j-1}_{\text{TX}}\right), \end{aligned} \tag{31}$$

and[5]

$$\begin{aligned} \beta(a_1,a_2) = &\Pr\left(\hat{W}_{\text{RX}_1}[j]=a_1|W_{\text{TX}}[j]=1,\mathbf{W}^{j-1}_{\text{TX}}\right) \\ &\times \Pr\left(\hat{W}_{\text{RX}_2}[j]=a_2|W_{\text{TX}}[j]=1,\mathbf{W}^{j-1}_{\text{TX}}\right). \end{aligned} \tag{32}$$

Proof: Please see Appendix D. ∎

Using Lemma 1, Lemma 2, and Lemma 3, we find that the equal distribution of molecules always achieves the local minimal error probability for SD-ML in a two-RX system, as stated in the following theorem:

Theorem 3: In the symmetric topology with two RXs, $Q_{\text{FC}}[j]$ achieves a local minimal value when $S_1 = \frac{N}{2}$ if $P_1 = \frac{1}{2}$.

Proof: Please see Appendix E. ∎

Remark 1: If all channel parameters are available offline and approximately constant during the whole transmission, then the optimization problem can be solved offline and the solution can be used to set the optimal molecule allocation among RXs for the entire transmission, as discussed in [32]. If some channel parameters are not available offline and may change, (e.g., distances between devices may change due to mobility, and the diffusion coefficient may vary over time and space), then the optimization problem could be solved by a controller device having higher computational capability than the RXs, as discussed in [33, 34]. The controller device can use estimation methods discussed in [35, 36] to obtain the channel parameters in the current symbol interval. It is reasonable to assume channel parameters remain constant during each symbol interval if the interval duration is sufficiently small. Once the controller device obtains the solution, it can be shared with the RXs to set the optimal molecule allocation for the emission in the current symbol interval.

[5]In the symmetric topology, $\sigma_1 = \sigma_2$ is valid because the observations at symmetric RXs are independently and identically distributed (even though symmetric RXs may not necessarily make the same decisions). We need to consider all possible realizations of $\hat{\mathbf{W}}^{j-1}_{\text{RX}_k}$ at each RX_k to evaluate $Q^{\sharp}_{\text{FC}}[j]$, but this requires high complexity. To facilitate the calculation, we only consider one realization of $\hat{\mathbf{W}}^{j-1}_{\text{RX}_k}$ at each RX and it is sufficiently accurate for the evaluation of $Q^{\sharp}_{\text{FC}}[j]$ to assume that this realization is the same for all RXs.

TABLE III
ENVIRONMENTAL PARAMETERS

Parameter	Symbol	Value
Volume of each RX	V_{RX_k}	$\frac{4}{3} \times \pi \times 0.2^3\ \mu\text{m}^3$
Radius of FC	r_{FC}	$0.2\,\mu$m
Time step at RXs	Δt_{RX}	$100\,\mu$s
Time step at FC	Δt_{FC}	$30\,\mu$s
Number of samples by RXs	M_{RX}	5
Number of samples by FC	M_{FC}	10
Transmission time interval	t_{trans}	1 ms
Report time interval	t_{report}	0.3 ms
Bit interval time	T	1.3 ms
Diffusion coefficient	$D_0 = D_k$	$5 \times 10^{-9}\text{m}^2/\text{s}$
Length of symbol sequence	L	20
Probability of binary 1	P_1	0.5

VI. NUMERICAL RESULTS AND SIMULATIONS

In this section, we present numerical and simulation results to examine the error performance of the ML detectors. We simulate using a particle-based method considered in [37], where we track the precise locations of all individual molecules. Unless otherwise noted, we consider the environmental parameters in Table III. Throughout this section, we keep the TX and the FC fixed at $(0\mu\text{m}, 0\mu\text{m}, 0\mu\text{m})$ and $(2\mu\text{m}, 0\mu\text{m}, 0\mu\text{m})$, respectively. To clearly demonstrate the impact of the number of samples and the number of RXs on the error probability of the system, we consider a symmetric topology in Section VI-A. To clearly show the impact of asymmetric RX location on the error probability of the system and the corresponding optimal molecule distribution, we consider an asymmetric topology in Section VI-B.

We assume that the TX releases 10^4 molecules for symbol "1". We also assume the total number of molecules released by all RXs for symbol "1" is *fixed* at 2000 throughout this section to ensure the fairness of error performance comparison for different K. For MD-ML and SD-ML, in Figs. 3-5, each RX releases $S_{\text{D}} = \lfloor 2000/K \rceil$ molecules to report a decision of "1". For SA-ML, in Figs. 3–5, each RX uses an amplification factor to ensure that the average number of molecules released by all RXs for transmission of one symbol is 1000 for the fair comparison among SA-ML, SD-ML, and MD-ML. $\overline{Q}_{\text{FC}}$ is obtained by averaging $Q_{\text{FC}}[j]$ over all symbol intervals and 50000 random-generated realizations of $\mathbf{W}_{\text{TX}}^{j-1}$, and then the value of $\overline{Q}_{\text{FC}}^*$ is the minimum $\overline{Q}_{\text{FC}}$ found by numerically optimizing the corresponding constant decision thresholds via exhaustive search. To decrease the complexity of exhaustive search, we consider the same decision threshold at all RXs such that $\xi_{\text{RX}_k} = \xi_{\text{RX}}, \forall k$.

In Figs. 3-5, for each ML detection variant, we plot the error probability with the local history and genie-aided history. We observe that the error performance using the local history has a very small degradation from that using the genie-aided history. This demonstrates the effectiveness of our proposed method to estimate the previous symbols. We also observe that the simulations have very strong agreement with the analytical results, thereby validating our analytical results. In Figs. 3-5, we observe that the error performance degradation with the local history compared to the genie-aided history for SA-ML is more noticeable than that for SD-ML and MD-ML. This is because in SD-ML and MD-ML, the FC directly estimates previous RX symbols from the RX-FC links. However, for SA-ML, the FC does not directly estimate the previous RX emissions from the RX-FC links and the error in the estimation of previous TX symbols propagates to the estimated previous RX emissions.

TABLE IV
SUMMARY OF CONSIDERED VARIANTS

Variants	Relaying at RXs	Molecule Type Used in RXs	Behavior at FC
Majority Rule [8, 9]	DF	Multiple	Constant Threshold
MD-ML	DF	Multiple	ML Detection
SD-Constant [10]	DF	Single	Constant Threshold
SD-ML	DF	Single	ML Detection
SA-Constant	AF	Single	Constant Threshold
SA-ML	AF	Single	ML Detection

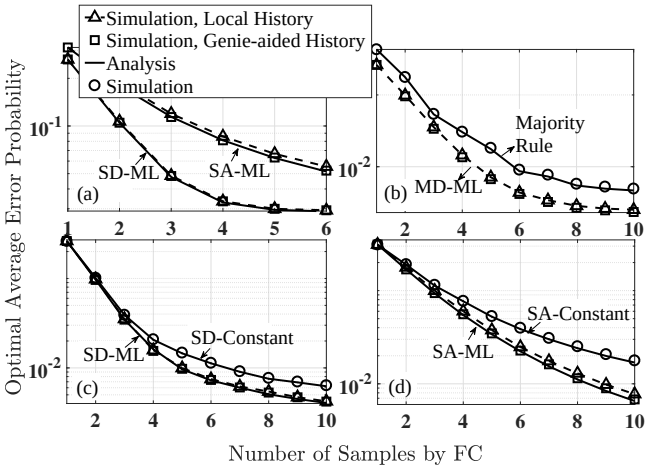

Fig. 3. Optimal average error probability $\overline{Q}_{\text{FC}}^*$ versus the number of samples by FC M_{FC} for (a) SD-ML and SA-ML, (b) MD-ML and the majority rule, (c) SD-ML and SD-Constant, and (d) SA-ML and SA-Constant. The analytical error performance of the majority rule and SD-Constant is presented in [9] and [10], respectively.

A. Symmetric Topology

We consider at most 6 RXs in this subsection and the specific locations of RXs are: $(2\mu\text{m}, \pm 0.6\mu\text{m}, 0)$ and $(2\mu\text{m}, \pm 0.3\mu\text{m}, \pm 0.5196\mu\text{m})$, where the RXs are placed on a circle perpendicular to the line passing from the TX, the FC, and the center of the circle.

In order to provide trade-offs between the performance versus the information available, we compare the error performance of the ML detectors with the majority rule [8, 9] and SD-Constant [10]. Notably, we also propose a *new* variant for comparison, namely, SA-Constant. In SA-Constant, the behavior of each RX is the same as that in SA-ML, but the FC makes a decision $\hat{W}_{\text{FC}}[j]$ by comparing $\tilde{s}[j]$ with a constant threshold ξ_{FC}, independent of $\mathbf{W}_{\text{TX}}^{j-1}$. It can be shown that $Q_{\text{FC}}[j]$ for SA-Constant with *any* realization of $\mathbf{W}_{\text{TX}}^{j-1}$ can be obtained by replacing $\xi_{\text{FC}}^{\text{ad,SA}}[j]$ with the threshold ξ_{FC} in (22). We summarize all variants considered in this subsection in Table IV. For these variants, we consider the same parameters as the ML detectors for the fairness of our comparisons.

In Fig. 3, we plot the optimal average global error probability $\overline{Q}_{\text{FC}}^*$ of different variants versus the number M_{FC} of samples by the FC. In Fig. 3, the report time interval is fixed at

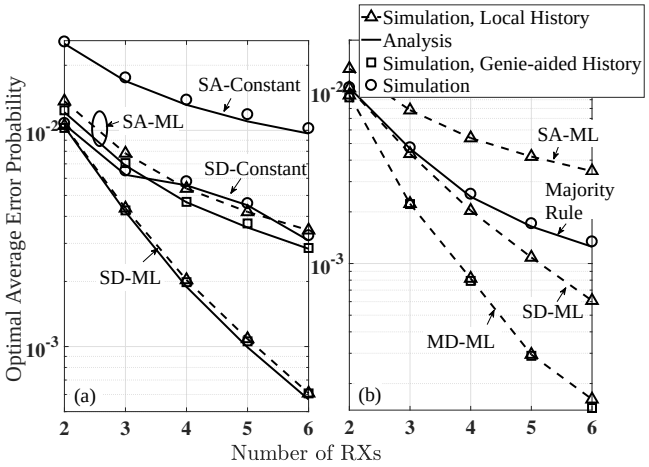

Fig. 4. Optimal average error probability $\overline{Q}^*_{\text{FC}}$ of different variants versus the number of RXs K. The analytical error performance of SD-Constant and the majority rule is presented in [10] and [9], respectively.

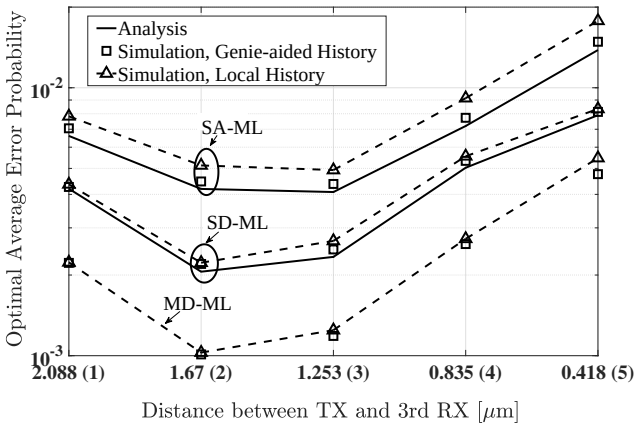

Fig. 5. Optimal average error probability $\overline{Q}^*_{\text{FC}}$ of different variants versus the distance d_{TX_3} between the TX and RX_3. RX_1 and RX_2 are fixed at $(2\mu\text{m}, 0, 0.6\mu\text{m})$ and $(2\mu\text{m}, 0, -0.6\mu\text{m})$, respectively. The locations of RX_3 are (1) $(2\mu\text{m}, 0.6\mu\text{m}, 0)$, (2) $(1.6\mu\text{m}, 0.48\mu\text{m}, 0)$, (3) $(1.2\mu\text{m}, 0.36\mu\text{m}, 0)$, (4) $(0.8\mu\text{m}, 0.24\mu\text{m}, 0)$, (5) $(0.4\mu\text{m}, 0.12\mu\text{m}, 0)$.

$t_{\text{report}} = 0.3\,\text{ms}$ as in Table III and the time step at the FC for each M_{FC} is $\Delta t_{\text{FC}} = 0.3\,\text{ms}/M_{\text{FC}}$. We observe that the system error performance improves as M_{FC} increases. This is because when M_{FC} increases, the number of molecules expected to be observed at each RX increases.

In Fig. 3(a), we consider a single-RX system (which is analogous to the two-hop environment considered in [31]). We observe that SD-ML outperforms SA-ML. In Fig. 3(b)-(d), we consider a three-RX system. We observe that MD-ML, SD-ML, and SA-ML outperform the majority rule, SD-Constant, and SA-Constant, respectively. However, the error performance degradation with these simpler cooperative variants are all within an order of magnitude for the range of M_{FC} considered. This demonstrates the relatively good performance of the simpler variants.

In Fig. 4, we plot the optimal average global error probability versus the number K of cooperative RXs for different variants. We see that the system error performance improves as K increases, even though the total number of molecules is constrained. The same observation of error performance improvement may be observed in a channel with additive signal dependent noise if our results can be well approximated by the Gaussian signal dependent noise model [38]. The system error performance does not always improve as K increases. This is because if we keep increasing K, the number of released molecules for each RX_k decreases, which leads to the $\text{RX}_k - \text{FC}$ link becoming unreliable. The system error performance would improve as the volume of the FC increases for the fixed K, since the FC can observe more molecules, but the volume of microorganisms cannot be easily altered.

In Fig. 4(a), we observe that SD-Constant and SA-ML using the local history achieve similar error performance. In Fig. 4(b), we observe that the majority rule has similar error performance with SD-ML and the majority rule outperforms SA-ML using the local history. These observations demonstrate the good performance of the majority rule, relative to SD-ML and SA-ML. Importantly, we observe that MD-ML outperforms SD-ML and SD-ML outperforms SA-ML. This is because the knowledge of individual $\tilde{s}_k[j]$ for each $\text{RX}_k - \text{FC}$ link in MD-ML improves detection performance over only knowing the sum $\tilde{s}[j]$ in SD-ML. Comparing to RX_k making a binary decision in the current symbol interval in SD-ML, RX_k in SA-ML amplifies the ISI at RX_k in the current symbol interval due to the previous TX symbols.

The system error performance in the subsection would degrade relative to the independent case if any of the links become dependent. This can be explained by a special case where all RXs overlap each other and thus have the same observations. Then, the error performance of this case would be the same as that of a cooperative system with $K = 1$.

B. Asymmetric Topology

In Fig. 5, we consider a three-RX system and plot the optimal average error probability of different variants versus the distance between the TX and RX_3. We keep the positions of RX_1 and RX_2 fixed and move RX_3 along the line segment between the symmetric position and the TX, as indicated in the caption. We observe for our three variants that the error performance first improves and then decreases as RX_3 moves toward the TX. This is because both the TX-RX_3 link and the RX_3-FC link contribute to the error performance of the system. When d_{TX_3} is relatively large, the system error performance is dominated by the TX-RX_3 link and this link becomes more reliable as d_{TX_3} decreases. For d_{TX_3} is relatively small, the system error performance is dominated by the RX_3-FC link, which becomes weaker when d_{TX_3} decreases. We also observe that MD-ML outperforms SD-ML and SD-ML outperforms SA-ML, which is consistent with our observations in Fig. 4(b).

In the following figures, we present results to assess the accuracy of our proposed optimization method in Section V. We denote the solution to problem (26) by $\mathbf{S}^\dagger = \{S_1^\dagger, S_2^\dagger, \ldots, S_K^\dagger\}$. We denote the optimal solution via exhaustive search by $\mathbf{S}^\star = \{S_1^\star, S_2^\star, \ldots, S_K^\star\}$.

In Fig. 6, we consider a two-RX system and plot the error probability of SD-ML versus the number of molecules released by RX_1 for different location of RX_1, where we keep RX_2 fixed at $(2\mu\text{m}, 0.6\mu\text{m}, 0\mu\text{m})$ and move RX_1 along the line segment between the symmetric position and the TX, as

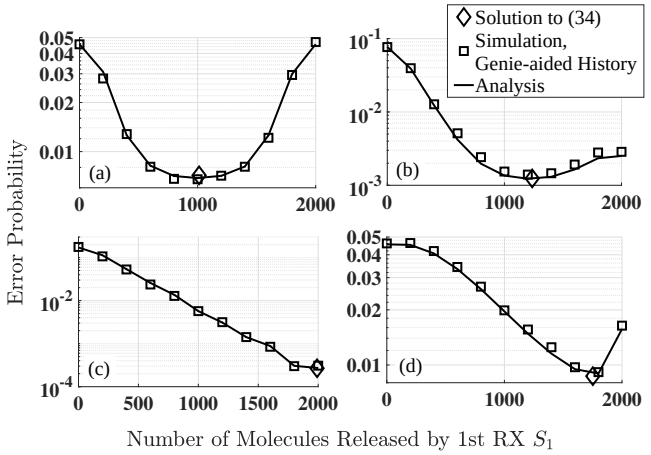

Fig. 6. Error probability $Q_{\text{FC}}[j]$ of SD-ML versus the number of molecules released by RX_1, S_1, for different locations of RX_1: (a) $(2\mu\text{m}, 0.6\mu\text{m}, 0\mu\text{m})$, (b) $(1.5\mu\text{m}, 0.45\mu\text{m}, 0\mu\text{m})$, (c) $(1\mu\text{m}, 0.3\mu\text{m}, 0\mu\text{m})$, (d) $(0.5\mu\text{m}, 0.15\mu\text{m}, 0\mu\text{m})$. The location of RX_2 is fixed at $(2\mu\text{m}, -0.6\mu\text{m}, 0\mu\text{m})$.

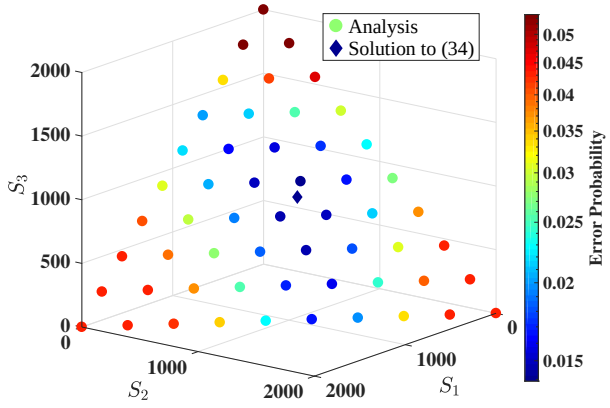

Fig. 7. Error probability $Q_{\text{FC}}[j]$ of SD-ML versus the number of molecules released by RX_1, S_1, the number of molecules released by RX_2, S_2, and the number of molecules released by RX_3, S_3. The X-axis, Y-axis, and Z-axis coordinates of '♦' are the solutions to problem (26). RX_1, RX_2, and RX_3 are at $(1.915\mu\text{m}, 0.58\mu\text{m}, 0)$, $(1.827\mu\text{m}, 0.579\mu\text{m}, 0)$, and $(1.265\mu\text{m}, 0.328\mu\text{m}, 0)$, respectively. The x-axis and y-axis coordinates of the locations of the RXs are randomly generated.

indicated in the caption. The x-axis coordinate of $\diamond$ is the solution $S_1^\dagger$ to (26) and the corresponding y-axis coordinate is the $Q_{\text{FC}}^\sharp[j]$ achieved at $\mathbf{S}^\dagger$. We observe that $S_1^\dagger$ and $Q_{\text{FC}}^\sharp[j]|_{\mathbf{S}=\mathbf{S}^\dagger}$ are almost identical to $S_1^\star$ and $Q_{\text{FC}}[j]|_{\mathbf{S}=\mathbf{S}^\star}$, respectively, which confirms the validity of Lemmas 1 and 2, the effectiveness of (26), and the accuracy of our method to solve (26). In Fig. 6(a), we observe that $S_1 = 1000$ achieves the minimal $Q_{\text{FC}}[j]$, which verifies Theorem 3. Interestingly, we observe that from Figs. 6(a)–(d), when we move RX_1 towards the TX, the optimal molecule allocation for RX_1 first increases and then decreases. This is because, when RX_1 approaches to the TX, the $\text{TX} - \text{RX}_1 - \text{FC}$ link becomes more reliable, so increasing the number of molecules for RX_1 optimizes the whole system; and when RX_1 is very close to the TX, the $\text{TX} - \text{RX}_1 - \text{FC}$ link becomes less reliable due to a weak $\text{RX}_1 - \text{FC}$ link. In particular, in Fig. 6(c), the optimal solution is to allocate all molecules to RX_1. This is because when RX_1 is at $(1\mu\text{m}, 0.3\mu\text{m}, 0\mu\text{m})$, RX_1 is very close to the optimal relay location, i.e., the midpoint between the TX and the FC, thus the $\text{TX} - \text{RX}_1 - \text{FC}$ link is much more reliable than the $\text{TX} - \text{RX}_2 - \text{FC}$ link and allocating all molecules to RX_1 optimizes the whole system.

In Fig. 7, we consider a three-RX system and plot the error probability of SD-ML versus the number of molecules released by RX_1, RX_2, and RX_3. The locations of the three RXs are generated randomly, as indicated in the caption. The x-axis, y-axis, and z-axis coordinates of '♦' are the solutions $S_1^\dagger$, $S_2^\dagger$, and $S_3^\dagger$ to problem (26), respectively. The corresponding 4th coordinate (i.e., color bar) is the $Q_{\text{FC}}^\sharp[j]$ achieved at $\mathbf{S}^\dagger$. We observe that $\mathbf{S}^\dagger$ and $Q_{\text{FC}}^\sharp[j]|_{\mathbf{S}=\mathbf{S}^\dagger}$ are almost identical to $\mathbf{S}^\star$ and $Q_{\text{FC}}[j]|_{\mathbf{S}=\mathbf{S}^\star}$, respectively, which again verifies Lemma 1, Lemma 2, and the effectiveness of problem (26).

VII. Conclusions

Combined with our initial work in [1], we presented for the first time symbol-by-symbol ML detection for the cooperative diffusion-based MC system with multiple communication phases. We considered the transmission of a sequence of binary symbols and accounted for the resultant ISI in the design and analysis of the system. We presented three ML detectors, i.e., MD-ML, SD-ML, and SA-ML. For practicality, the FC chooses the current symbol using its own local history. For tractability, we derived the system error probabilities for SD-ML and SA-ML using the genie-aided history. We formulated and solved a multi-dimensional optimization problem to find the optimal molecule allocation among RXs that minimizes the system error probability of SD-ML. We analytically proved that the equal distribution of molecules among two symmetric RXs obtains the local minimal error probability of SD-ML. Using numerical and simulation results, we corroborated the accuracy of these analytical expressions and the effectiveness of the formulated optimization problem. Our results revealed trade-offs between the performance, knowledge of previous symbols, the types of molecule, relaying modes, and computational complexity.

Appendix A
Proof of Theorem 1

We first prove the decision rule for SD-ML when $\hat{\lambda}_{\text{I}}^{\text{D}}[j] > 0$. To this end, based on (4), we first rewrite the general decision rule for SD-ML as $\hat{W}_{\text{FC}}[j] = 1$ if $\frac{\mathcal{L}_1^{\text{SD}}[j]}{\mathcal{L}_0^{\text{SD}}[j]} \geq 1$, otherwise $\hat{W}_{\text{FC}}[j] = 0$. Thus, if $\frac{\mathcal{L}_1^{\text{SD}}[j]}{\mathcal{L}_0^{\text{SD}}[j]}$ is a monotonically increasing function with respect to $\tilde{s}[j]$, then we can obtain the decision rule. We can prove that $\frac{\mathcal{L}_1^{\text{SD}}[j]}{\mathcal{L}_0^{\text{SD}}[j]}$ is a monotonically increasing function with respect to $\tilde{s}[j]$ by proving that $\left(\frac{\mathcal{L}_1^{\text{SD}}[j]}{\mathcal{L}_0^{\text{SD}}[j]}\right)' > 0$. Based on (13), we first rewrite $\mathcal{L}_1^{\text{SD}}[j]$ and $\mathcal{L}_0^{\text{SD}}[j]$ as

$$\mathcal{L}_1^{\text{SD}}[j] = \sum_{h_1=1}^{2^K} \Big[\Pr(h_1|1) \exp\left(-\hat{\lambda}_{\text{I}}^{\text{D}}[j] - \hat{\lambda}_{\text{s},h_1}^{\text{D,tot}}[j]\right) \times \left(\hat{\lambda}_{\text{I}}^{\text{D}}[j] + \hat{\lambda}_{\text{s},h_1}^{\text{D,tot}}[j]\right)^{\tilde{s}[j]} \left(\tilde{s}[j]!\right)^{-1} \Big] \tag{33}$$

and

$$\mathcal{L}_0^{\text{SD}}[j] = \sum_{h_0=1}^{2^K} \Big[\Pr(h_0|0) \exp\left(-\hat{\lambda}_{\text{I}}^{\text{D}}[j] - \hat{\lambda}_{\text{s},h_0}^{\text{D,tot}}[j]\right) \times \left(\hat{\lambda}_{\text{I}}^{\text{D}}[j] + \hat{\lambda}_{\text{s},h_0}^{\text{D,tot}}[j]\right)^{\tilde{s}[j]} (\tilde{s}[j]!)^{-1} \Big], \quad (34)$$

respectively, where $\Pr(h|b) = \Pr\left(\hat{\mathcal{W}}_{j,h}^{\text{RX}} | W_{\text{TX}}[j] = b, \mathbf{W}_{\text{TX}}^{j-1}\right)$. Based on (33) and (34), we find the first derivative of $\frac{\mathcal{L}_1^{\text{SD}}[j]}{\mathcal{L}_0^{\text{SD}}[j]}$ with respect to $\tilde{s}[j]$ as

$$\left(\frac{\mathcal{L}_1^{\text{SD}}[j]}{\mathcal{L}_0^{\text{SD}}[j]}\right)' = \sum_{h_1=1}^{2^K} \sum_{h_0=1}^{2^K} \frac{[\Pr(h_1|1)\Pr(h_0|0)\,\Pi(h_1,h_0)]}{\left(\mathcal{L}_0^{\text{SD}}[j](\tilde{s}[j]!)\right)^2}, \quad (35)$$

where

$$\Pi(h_1,h_0) = \exp\left(-2\hat{\lambda}_{\text{I}}^{\text{D}}[j] - \hat{\lambda}_{\text{s},h_1}^{\text{D,tot}}[j] - \hat{\lambda}_{\text{s},h_0}^{\text{D,tot}}[j]\right) \times \left(\hat{\lambda}_{\text{I}}^{\text{D}}[j] + \hat{\lambda}_{\text{s},h_0}^{\text{D,tot}}[j]\right)^{\tilde{s}[j]} \left(\hat{\lambda}_{\text{I}}^{\text{D}}[j] + \hat{\lambda}_{\text{s},h_1}^{\text{D,tot}}[j]\right)^{\tilde{s}[j]} \times \log\left(\frac{\hat{\lambda}_{\text{I}}^{\text{D}}[j] + \hat{\lambda}_{\text{s},h_1}^{\text{D,tot}}[j]}{\hat{\lambda}_{\text{I}}^{\text{D}}[j] + \hat{\lambda}_{\text{s},h_0}^{\text{D,tot}}[j]}\right). \quad (36)$$

We observe that in (35), all terms are positive except for the $\log(\cdot)$ term. Since $\log(x) > 0$ when $x > 1$, we separate (35) into two parts: $\log(\cdot) > 0$ and $\log(\cdot) < 0$. By doing so, we rewrite (35) as the sum of A and B, i.e.,

$$A = \sum_{h_1=1}^{2^K} \sum_{h_0=1,\, \hat{\lambda}_{\text{s},h_1}^{\text{D,tot}}[j] > \hat{\lambda}_{\text{s},h_0}^{\text{D,tot}}[j]}^{2^K} \frac{[\Pr(h_1|1)\Pr(h_0|0)\,\Pi(h_1,h_0)]}{\left(\mathcal{L}_0^{\text{SD}}[j](\tilde{s}[j]!)\right)^2} \quad (37)$$

and

$$B = \sum_{h_1=1}^{2^K} \sum_{h_0=1,\, \hat{\lambda}_{\text{s},h_1}^{\text{D,tot}}[j] < \hat{\lambda}_{\text{s},h_0}^{\text{D,tot}}[j]}^{2^K} \frac{[\Pr(h_1|1)\ \Pr(h_0|0)\,\Pi(h_1,h_0)]}{\left(\mathcal{L}_0^{\text{SD}}[j](\tilde{s}[j]!)\right)^2}. \quad (38)$$

We further rearrange the summation orders and exchange h_1 and h_0 in (38) to rewrite B as

$$B = \sum_{h_1=1}^{2^K} \sum_{h_0=1,\, \hat{\lambda}_{\text{s},h_1}^{\text{D,tot}}[j] > \hat{\lambda}_{\text{s},h_0}^{\text{D,tot}}[j]}^{2^K} \frac{[\Pr(h_0|1)\ \Pr(h_1|0)\,\Pi(h_0,h_1)]}{\left(\mathcal{L}_0^{\text{SD}}[j](\tilde{s}[j]!)\right)^2}. \quad (39)$$

Combining (37) and (39) and applying $\Pi(h_1,h_0) = -\Pi(h_0,h_1)$, we have

$$\left(\frac{\mathcal{L}_1^{\text{SD}}[j]}{\mathcal{L}_0^{\text{SD}}[j]}\right)' = \sum_{h_1=1}^{2^K} \sum_{h_0=1,\, \hat{\lambda}_{\text{s},h_1}^{\text{D,tot}}[j] > \hat{\lambda}_{\text{s},h_0}^{\text{D,tot}}[j]}^{2^K} \frac{[\vartheta(h_1,h_0)\Pi(h_1,h_0)]}{\left(\mathcal{L}_0^{\text{SD}}[j](\tilde{s}[j]!)\right)^2}, \quad (40)$$

where $\vartheta(h_1,h_0) = \Pr(h_1|1)\Pr(h_0|0) - \Pr(h_0|1)\Pr(h_1|0)$. We find that (40) > 0 holds when $\vartheta(h_1,h_0) > 0$ is valid, i.e., where $\hat{\lambda}_{\text{s},h_1}^{\text{D,tot}}[j] > \hat{\lambda}_{\text{s},h_0}^{\text{D,tot}}[j]$. We note that $\hat{\lambda}_{\text{s},h_1}^{\text{D,tot}}[j] > \hat{\lambda}_{\text{s},h_0}^{\text{D,tot}}[j]$ leads to $\| \hat{\mathcal{W}}_{j,h_1}^{\text{RX}} \|_1 > \| \hat{\mathcal{W}}_{j,h_0}^{\text{RX}} \|_1$, where $\| \mathbf{x} \|_1$ is the 1-norm of the vector $\mathbf{x}$. When $\| \hat{\mathcal{W}}_{j,h_1}^{\text{RX}} \|_1 > \| \hat{\mathcal{W}}_{j,h_0}^{\text{RX}} \|_1$ holds, we have $\Pr(h_1|1) > \Pr(h_0|1)$ and $\Pr(h_0|0) > \Pr(h_1|0)$, which leads to $\vartheta(h_1,h_0) > 0$. Thus, $\vartheta(h_1,h_0) > 0$ holds if $\hat{\lambda}_{\text{s},h_1}^{\text{D,tot}}[j] > \hat{\lambda}_{\text{s},h_0}^{\text{D,tot}}[j]$. This proves that $\left(\frac{\mathcal{L}_1^{\text{SD}}[j]}{\mathcal{L}_0^{\text{SD}}[j]}\right)' > 0$ and thus proves the decision rule for SD-ML when $\hat{\lambda}_{\text{I}}^{\text{D}}[j] > 0$.

We finally prove the decision rule when $\hat{\lambda}_{\text{I}}^{\text{D}}[j] = 0$. We recall that $\hat{\lambda}_{\text{I}}^{\text{D}}[j] = 0$ means all previous RX symbols are "0". It probably occurs when all previous TX symbols are "0" (i.e., no ISI at RX_k) if the error probability of the first phase is small. Hence, there is no likelihood that "1" is detected at RX_k when "0" is transmitted by the TX, which leads to $\Pr\left(\hat{\mathcal{W}}_{j,h}^{\text{RX}} = \mathbf{0} | W_{\text{TX}}[j] = 0, \mathbf{W}_{\text{TX}}^{j-1}\right) \approx 1$ and $\Pr\left(\hat{\mathcal{W}}_{j,h}^{\text{RX}} \neq \mathbf{0} | W_{\text{TX}}[j] = 0, \mathbf{W}_{\text{TX}}^{j-1}\right) \approx 0$. Using these approximations and $\hat{\lambda}_{\text{I}}^{\text{D}}[j] = 0$, we have $\mathcal{L}_0^{\text{SD}}[j] \approx \exp(0)\,(0)^{\tilde{s}[j]}$. When $\hat{\lambda}_{\text{I}}^{\text{A}}[j] = 0$ and $\tilde{s}[j] = 0$, $\mathcal{L}_0^{\text{SD}}[j]$ is 1, thus the decision at the FC is always $\hat{W}_{\text{FC}}[j] = 0$ since $\mathcal{L}_1^{\text{SD}}[j] < 1$. When $\hat{\lambda}_{\text{I}}^{\text{A}}[j] = 0$ and $\tilde{s}[j] > 0$, $\mathcal{L}_0^{\text{SD}}[j]$ is 0, thus the decision at the FC is always $\hat{W}_{\text{FC}}[j] = 1$ since $\mathcal{L}_1^{\text{SD}}[j] > 0$.

APPENDIX B
PROOF OF LEMMA 2

We take the first derivative of (24) with respect to ξ. However, $Q_{\text{FC}}^{\sharp}[j]$ is a discrete function with respect to ξ, which makes $Q_{\text{FC}}^{\sharp}[j]$ not differentiable in terms of ξ. To tackle this challenge, we approximate the sum in (25) with an integral with respect to η, i.e.,

$$\Lambda \approx \int_{\eta=0}^{\xi} \exp\left(-\hat{\lambda}_{\text{I}}^{\text{D}}[j] - \hat{\lambda}_{\text{s},h}^{\text{D,tot}}[j]\right) \frac{\left(\hat{\lambda}_{\text{I}}^{\text{D}}[j] + \hat{\lambda}_{\text{s},h}^{\text{D,tot}}[j]\right)^{\eta}}{(\eta!)} d\eta. \quad (41)$$

Using the continuous approximation of Λ in (41) and $\partial \int_{t=0}^{x} f(t)dt / \partial x = f(x)$, we take the first derivative of (24) with respect to ξ as $\partial Q_{\text{FC}}^{\sharp}[j] / \partial \xi = P_1\psi_1(\xi) - (1-P_1)\psi_2(\xi)$, where $\psi_b(\xi)$, $b \in \{0,1\}$, is given by

$$\psi_b(\xi) = \sum_{h=1}^{2^K} \Big[\Pr\left(\hat{\mathcal{W}}_{j,h}^{\text{RX}} | W_{\text{TX}}[j] = b, \mathbf{W}_{\text{TX}}^{j-1}\right) (\xi!)^{-1} \times \exp\left(-\hat{\lambda}_{\text{I}}^{\text{D}}[j] - \hat{\lambda}_{\text{s},h}^{\text{D,tot}}[j]\right) \left(\hat{\lambda}_{\text{I}}^{\text{D}}[j] + \hat{\lambda}_{\text{s},h}^{\text{D,tot}}[j]\right)^{\xi} \Big]. \quad (42)$$

Comparing (42) with (13), we find that $\psi_b(\tilde{s}[j]) = \mathcal{L}_b^{\text{SD}}[j]$. We recall that $\xi_{\text{FC}}^{\text{ad,SD}}[j]$ is the solution to $\mathcal{L}_1^{\text{SD}}[j] = \mathcal{L}_0^{\text{SD}}[j]$ in terms of $\tilde{s}[j]$. Hence, $\xi_{\text{FC}}^{\text{ad,SD}}[j]$ is the solution to $P_1\psi_1(\xi) - (1-P_1)\psi_2(\xi) = \partial Q_{\text{FC}}^{\sharp}[j] / \partial \xi = 0$ if $P_1 = \frac{1}{2}$. Therefore, $\xi_{\text{FC}}^{\text{ad,SD}}[j]$ is the optimal ξ which minimizes (24).

APPENDIX C
PROOF OF PROPOSITION 1

The problem (26) has $K+1$ optimization variables and the evaluation of its Hessian requires very high computational complexity. To decrease the complexity, we first consider the simplest case with $K = 2$ and investigate the Hessian of $Q_{\text{FC}}^{\sharp}[j]$ with respect to S_1 for a fixed ξ. To this end, we take the first derivative of $Q_{\text{FC}}^{\sharp}[j]$ with respect to S_1. In (24), Λ is a discrete function in terms of S_1, which makes the derivative cumbersome. If we approximate Λ using (41), there is no closed-form for the first derivative of (41) with respect to S_1. To overcome this challenge, we approximate Λ by another continuous approximation, i.e., the continuous

regularized incomplete Gamma function. By doing so, we have $\Lambda \approx \Gamma\left(\lceil\xi\rceil, \hat{\lambda}_{\mathrm{I}}^{\mathrm{D}}[j] + \hat{\lambda}_{\mathrm{s},h}^{\mathrm{D,tot}}[j]\right)/\Gamma\left(\lceil\xi\rceil\right)$, where $\Gamma(\gamma,\delta)$ is the incomplete Gamma function and the Gamma function $\Gamma(\gamma)$ is a special case of $\Gamma(\gamma,\delta)$ with $\delta = 0$. Applying this approximation to (24), we obtain the continuous approximation of $Q_{\mathrm{FC}}^{\sharp}[j]$. Using $\partial\Gamma(\gamma,\delta)/\partial\delta = -\exp(-\delta)\,\delta^{\gamma-1}$, we take the first derivative of $Q_{\mathrm{FC}}^{\sharp}[j]$ as

$$\frac{\partial\, Q_{\mathrm{FC}}^{\sharp}[j]}{\partial\, S_1} \approx \frac{1}{\Gamma\left(\lceil\xi\rceil\right)}\Bigg(\sum_{a_1=0}^{1}\sum_{a_2=0}^{1}\left((1-P_1)\,\alpha(a_1,a_2) - P_1\beta(a_1,a_2)\right)\exp\left(-\Xi(a_1,a_2)\right) \times \left(\Xi(a_1,a_2)\right)^{-1+\lceil\xi\rceil}\Omega(a_1,a_2)\Bigg), \tag{43}$$

where $\Xi(a_1,a_2) = \sigma_1 S_1 + \sigma_2(N-S_1) + a_1\nu_1 S_1 + a_2\nu_2(N-S_1)$ and $\Omega(a_1,a_2) = \sigma_1 - \sigma_2 + a_1\nu_1 - a_2\nu_2$, where σ_k and ν_k are given in (29) and (30), respectively. We then find the second derivative of $Q_{\mathrm{FC}}^{\sharp}[j]$ with respect to S_1 as

$$\frac{\partial^2 Q_{\mathrm{FC}}^{\sharp}[j]}{\partial {S_1}^2} = -\frac{1}{\Gamma\left(\lceil\xi\rceil\right)}\Bigg(\sum_{a_1=0}^{1}\sum_{a_2=0}^{1}\exp\left(-\Xi(a_1,a_2)\right) \times \left(\Xi(a_1,a_2)\right)^{-2+\lceil\xi\rceil}\left(\Omega(a_1,a_2)\right)^2\varpi\Bigg), \tag{44}$$

where

$$\varpi = \left((1-P_1)\,\alpha(a_1,a_2) - P_1\beta(a_1,a_2)\right)\left(1-\lceil\xi\rceil+\Xi(a_1,a_2)\right). \tag{45}$$

In (44), all terms are nonnegative except for ϖ. Thus, if $\varpi > 0$ holds for each summand, (44) is nonnegative. However, the condition $\varpi > 0$ is not always valid for $a_1 \in \{0,1\}$ and $a_2 \in \{0,1\}$. Thus, for a fixed ξ, $\partial^2 Q_{\mathrm{FC}}^{\sharp}[j]/\partial\xi^2$ is not always nonnegative, which means that the Hessian of $Q_{\mathrm{FC}}^{\sharp}[j]$ with respect to $\mathbf{S}$ and ξ is not always positive semidefinite.

APPENDIX D
PROOF OF LEMMA 3

Using (28), we simplify (43) as

$$\frac{\partial\, Q_{\mathrm{FC}}^{\sharp}[j]}{\partial\, S_1} = \frac{\exp(-\Phi_1 - 2\nu S_1)}{\Phi_1\Phi_2\Gamma\left(\lceil\xi\rceil\right)}\left(\alpha(P_1-1)+\beta P_1\right)\nu \times\left(\exp(2\nu S_1)\Phi_1^{\lceil\xi\rceil}\Phi_2 - \exp(N\nu)\Phi_2^{\lceil\xi\rceil}\Phi_1\right), \tag{46}$$

where $\Phi_1 = N(\nu+\sigma) - \nu S_1$ and $\Phi_2 = N\sigma + \nu S_1$. It can be shown that $S_1 = \frac{N}{2}$ is the one of the solutions of (46). Hence, $Q_{\mathrm{FC}}^{\sharp}[j]$ has a local minimum or maximum when $S_1 = \frac{N}{2}$. We then apply (28) and $S_1 = \frac{N}{2}$ to (44) to obtain the second derivative of $Q_{\mathrm{FC}}^{\sharp}[j]$ at $S_1 = \frac{N}{2}$. By doing so, we have

$$\frac{\partial^2 Q_{\mathrm{FC}}^{\sharp}[j]}{\partial {S_1}^2}\Big|_{S_1=\frac{N}{2}} = \frac{4\exp(-\frac{1}{2}N(\nu+2\sigma))}{N^2(\nu+2\sigma)^2\Gamma\left(\lceil\xi\rceil\right)} \times \nu^2\left(\frac{N(\nu+2\sigma)}{2}\right)^{\lceil\xi\rceil}\Upsilon(\xi), \tag{47}$$

where all terms are nonnegative except for $\Upsilon(\xi)$. Hence if $\Upsilon(\xi) > 0$, (47) is nonnegative and $Q_{\mathrm{FC}}^{\sharp}[j]$ achieves a local minimum at $S_1 = \frac{N}{2}$; otherwise, it achieves a local maximum.

APPENDIX E
PROOF OF THEOREM 3

Based on Lemma 3, $Q_{\mathrm{FC}}^{\sharp}[j]$ achieves a local minimal value at $S_1 = \frac{N}{2}$ when $\Upsilon(\xi) > 0$. Based on Lemma 1, the approximation of $Q_{\mathrm{FC}}[j]$ by $Q_{\mathrm{FC}}^{\sharp}[j]$ is tight when $\xi = \xi_{\mathrm{FC}}^{\mathrm{ad,SD}}[j]$. Thus, we can prove that $Q_{\mathrm{FC}}[j]$ always achieves a local minimal value at $S_1 = \frac{N}{2}$ by proving that $\Upsilon(\xi) > 0$ always holds when $\xi = \xi_{\mathrm{FC}}^{\mathrm{ad,SD}}[j]$. That is to say, we need to prove $\Upsilon(\xi_{\mathrm{FC}}^{\mathrm{ad,SD}}[j]) > 0$. Based on the proof of Lemma 2, we also recall that $\xi_{\mathrm{FC}}^{\mathrm{ad,SD}}[j]$ is the solution to $P_1\psi_1(\xi) - (1-P_1)\psi_2(\xi) = \partial\, Q_{\mathrm{FC}}^{\sharp}[j]/\partial\,\xi = 0$ if $P_1 = \frac{1}{2}$. Thus, $\xi_{\mathrm{FC}}^{\mathrm{ad,SD}}[j]$ satisfies the condition: $\psi_1(\xi_{\mathrm{FC}}^{\mathrm{ad,SD}}[j]) - \psi_2(\xi_{\mathrm{FC}}^{\mathrm{ad,SD}}[j]) = 0$. Applying $S_1 = N/2$ to (42), we write $\psi_b(\xi_{\mathrm{FC}}^{\mathrm{ad,SD}}[j])$, where $b \in \{0,1\}$, using ν and σ as

$$\begin{aligned}
&\psi_b(\xi_{\mathrm{FC}}^{\mathrm{ad,SD}}[j]) \\
&= \left(\xi_{\mathrm{FC}}^{\mathrm{ad,SD}}[j]!\right)^{-1}\Bigg[\Pr(0,0|b)\,\exp(-\sigma N)\,(\sigma N)^{\xi_{\mathrm{FC}}^{\mathrm{ad,SD}}[j]} \\
&\quad + \Pr(0,1|b)\exp\left(-\sigma N - \frac{\nu N}{2}\right)\left(\sigma N + \frac{\nu N}{2}\right)^{\xi_{\mathrm{FC}}^{\mathrm{ad,SD}}[j]} \\
&\quad + \Pr(1,0|b)\exp\left(-\sigma N - \frac{\nu N}{2}\right)\left(\sigma N + \frac{\nu N}{2}\right)^{\xi_{\mathrm{FC}}^{\mathrm{ad,SD}}[j]} \\
&\quad + \Pr(1,1|b)\exp(-\sigma N - \nu N)\,(\sigma N + \nu N)^{\xi_{\mathrm{FC}}^{\mathrm{ad,SD}}[j]}\Bigg],
\end{aligned} \tag{48}$$

where $\Pr\left(\hat{\mathcal{W}}_{j,h}^{\mathrm{RX}}|b\right) = \Pr\left(\hat{\mathcal{W}}_{j,h}^{\mathrm{RX}}|W_{\mathrm{TX}}[j]=b, \mathbf{W}_{\mathrm{TX}}^{j-1}\right)$. In (48), we have $\Pr(0,1|0) = \Pr(1,0|0) = \alpha$ and $\Pr(0,1|1) = \Pr(1,0|1) = \beta$ based on (28). We then approximate $\Pr(0,0|0) = \Pr(1,1|1) \approx 1$ and $\Pr(0,0|1) = \Pr(1,1|0) \approx 0$, which is tight when the error probability of the $\mathrm{TX}-\mathrm{RX}_k$ link is small. Using these approximations, α, and β, we rewrite $\psi_0(\xi_{\mathrm{FC}}^{\mathrm{ad,SD}}[j])$ and $\psi_1(\xi_{\mathrm{FC}}^{\mathrm{ad,SD}}[j])$ as

$$\begin{aligned}
\psi_0(\xi_{\mathrm{FC}}^{\mathrm{ad,SD}}[j]) \approx{}& \left(\xi_{\mathrm{FC}}^{\mathrm{ad,SD}}[j]!\right)^{-1}\exp(-\sigma N)\,(\sigma N)^{\xi_{\mathrm{FC}}^{\mathrm{ad,SD}}[j]} \\
&+ 2\alpha\left(\xi_{\mathrm{FC}}^{\mathrm{ad,SD}}[j]!\right)^{-1}\exp\left(-\sigma N - \frac{\nu N}{2}\right) \\
&\times\left(\sigma N + \frac{\nu N}{2}\right)^{\xi_{\mathrm{FC}}^{\mathrm{ad,SD}}[j]}
\end{aligned} \tag{49}$$

and

$$\begin{aligned}
\psi_1(\xi_{\mathrm{FC}}^{\mathrm{ad,SD}}[j]) \approx{}& \left(\xi_{\mathrm{FC}}^{\mathrm{ad,SD}}[j]!\right)^{-1}\exp(-\sigma N - \nu N) \\
&\times(\sigma N + \nu N)^{\xi_{\mathrm{FC}}^{\mathrm{ad,SD}}[j]} + 2\beta\left(\xi_{\mathrm{FC}}^{\mathrm{ad,SD}}[j]!\right)^{-1} \\
&\times\exp\left(-\sigma N - \frac{\nu N}{2}\right)\left(\sigma N + \frac{\nu N}{2}\right)^{\xi_{\mathrm{FC}}^{\mathrm{ad,SD}}[j]},
\end{aligned} \tag{50}$$

respectively. Using $\psi_1(\xi_{\mathrm{FC}}^{\mathrm{ad,SD}}[j]) - \psi_2(\xi_{\mathrm{FC}}^{\mathrm{ad,SD}}[j]) = 0$ and some basic manipulations, we obtain

$$\begin{aligned}
\beta - \alpha = \frac{1}{2}\exp\left(-\frac{\nu N}{2}\right)&\left(\frac{\sigma N + \nu N}{\sigma N + \frac{\nu N}{2}}\right)^{\xi_{\mathrm{FC}}^{\mathrm{ad,SD}}[j]} \\
&\times\left(\exp(\nu N)\left(\frac{\sigma N}{\sigma N + \nu N}\right)^{\xi_{\mathrm{FC}}^{\mathrm{ad,SD}}[j]} - 1\right).
\end{aligned} \tag{51}$$

Applying (51) and $P_1 = \frac{1}{2}$ to (27), we have $\Upsilon(\xi_{\text{FC}}^{\text{ad,SD}}[j]) = \frac{\theta_1\theta_2}{4}\exp\left(-\frac{\nu N}{2}\right)\left(\frac{\sigma N+\nu N}{\sigma N+\frac{\nu N}{2}}\right)^{\xi_{\text{FC}}^{\text{ad,SD}}[j]}$, where $\theta_1 = \left(\exp\left(\nu N\right)\left(\sigma N/(\sigma N+\nu N)\right)^{\xi_{\text{FC}}^{\text{ad,SD}}[j]}-1\right)$ and $\theta_2 = \left(2+N(\nu+2\sigma)-2\xi_{\text{FC}}^{\text{ad,SD}}[j]\right)$. To prove $\Upsilon(\xi_{\text{FC}}^{\text{ad,SD}}[j]) > 0$, we only need to prove $\theta_1\theta_2 > 0$, since all other terms in Υ are nonnegative. If $\theta_1 > 0$, we have $\xi_{\text{FC}}^{\text{ad,SD}}[j] < \nu N/\log\left((\sigma N+\nu N)/\nu N\right)$. Applying $\log(x) \leq x-1$, where $x > 0$, we further lower-bound $\xi_{\text{FC}}^{\text{ad,SD}}[j]$ by $\xi_{\text{FC}}^{\text{ad,SD}}[j] < \sigma N$, which leads to $\theta_2 > 0$. If $\theta_1 < 0$, we have $\xi_{\text{FC}}^{\text{ad,SD}}[j] > \nu N/\log\left((\sigma N+\nu N)/\nu N\right)$. Applying $\log(x) \geq 1-1/x$, where $x > 0$, we further upper-bound $\xi_{\text{FC}}^{\text{ad,SD}}[j]$ by $\xi_{\text{FC}}^{\text{ad,SD}}[j] > (\sigma N+\nu N)$, which leads to $\theta_2 < 0$ if $\nu N/2 > 1$. Although the validity of $\nu N/2 > 1$ depends on the value of ν and N, it is generally valid. This is because $\nu N/2 > 1$ means that at least one signaling molecule is expected at the FC if the decision at RX_k is "1" and it is a reasonable condition to be satisfied. Since θ_1 and θ_2 are always both negative or positive, $\theta_1\theta_2 > 0$ holds, which leads to $\Upsilon(\xi_{\text{FC}}^{\text{ad,SD}}[j]) > 0$. Therefore, $Q_{\text{FC}}[j]$ achieves a local minimum at $S_1 = N/2$ when $K = 2$ in a symmetric topology.

REFERENCES

[1] Y. Fang, A. Noel, N. Yang, A. W. Eckford, and R. A. Kennedy, "Maximum likelihood detection for cooperative molecular communication," in *Proc. IEEE ICC*, May 2018, pp. 1–7.

[2] N. Farsad, H. B. Yilmaz, A. Eckford, C. B. Chae, and W. Guo, "A comprehensive survey of recent advancements in molecular communication," *IEEE Commun. Surveys Tuts.*, vol. 18, no. 3, pp. 1887–1919, Aug. 2016.

[3] T. Nakano and J. Q. Liu, "Design and analysis of molecular relay channels: An information theoretic approach," *IEEE Trans. Nanobiosci.*, vol. 9, no. 3, pp. 213–221, Sep. 2010.

[4] B. Atakan and O. B. Akan, "On molecular multiple-access, broadcast, and relay channels in nanonetworks," in *Proc. ICST BIONETICS*, Nov. 2008, pp. 16:1–16:8.

[5] T. Nakano, Y. Okaie, and A. V. Vasilakos, "Transmission rate control for molecular communication among biological nanomachines," *IEEE J. Select. Areas Commun.*, vol. 31, no. 12, pp. 835–846, Dec. 2013.

[6] C. T. Chou, "Extended master equation models for molecular communication networks," *IEEE Trans. Nanobiosci.*, vol. 12, no. 2, pp. 79–92, June 2013.

[7] B. H. Koo, C. Lee, H. B. Yilmaz, N. Farsad, A. W. Eckford, and C.-B. Chae, "Molecular MIMO: From theory to prototype," *IEEE J. Select. Areas Commun.*, vol. 34, no. 3, pp. 600–614, Mar. 2016.

[8] Y. Fang, A. Noel, N. Yang, A. W. Eckford, and R. A. Kennedy, "Distributed cooperative detection for multi-receiver molecular communication," in *Proc. IEEE GLOBECOM*, Dec. 2016, pp. 1–7.

[9] ——, "Convex optimization of distributed cooperative detection in multi-receiver molecular communication," *IEEE Trans. Mol. Bio. Multi-Scale Commun.*, vol. 3, no. 3, pp. 166–182, Sep. 2017.

[10] Y. Fang, A. Noel, Y. Wang, and N. Yang, "Simplified cooperative detection for multi-receiver molecular communication," in *Proc. IEEE ITW*, Nov. 2017, pp. 1–5.

[11] J. G. Proakis, *Digital Communication*, 4th ed. New York: McGraw-Hill, 2000.

[12] D. Kilinc and O. B. Akan, "Receiver design for molecular communication," *IEEE J. Select. Areas Commun.*, vol. 31, no. 12, pp. 705–714, Dec. 2013.

[13] A. Noel, K. C. Cheung, and R. Schober, "Optimal receiver design for diffusive molecular communication with flow and additive noise," *IEEE Trans. Nanobiosci.*, vol. 13, no. 3, pp. 350–362, Sept. 2014.

[14] M. U. Mahfuz *et al.*, "A comprehensive analysis of strength-based optimum signal detection in concentration-encoded molecular communication with spike transmission," *IEEE Trans. Nanobiosci.*, vol. 14, no. 1, pp. 67–83, Jan. 2015.

[15] A. Singhal, R. K. Mallik, and B. Lall, "Performance analysis of amplitude modulation schemes for diffusion-based molecular communication," *IEEE Trans. Wireless Commun.*, vol. 14, no. 10, pp. 5681–5691, Oct. 2015.

[16] S. Ghavami and F. Lahouti, "Abnormality detection in correlated gaussian molecular nano-networks: Design and analysis," *IEEE Trans. Nanobiosci.*, vol. 16, no. 3, pp. 189–202, Apr. 2017.

[17] T. C. Mai, M. Egan, T. Q. Duong, and M. D. Renzo, "Event detection in molecular communication networks with anomalous diffusion," *IEEE Commun. Lett.*, vol. 21, no. 6, pp. 1249–1252, June 2017.

[18] R. Mosayebi, V. Jamali, N. Ghoroghchian, R. Schober, M. Nasiri-Kenari, and M. Mehrabi, "Cooperative abnormality detection via diffusive molecular communications," *IEEE Trans. Nanobiosci.*, vol. 16, no. 8, pp. 828–842, Dec. 2017.

[19] U. Rogers and M. S. Koh, "Parallel molecular distributed detection with brownian motion," *IEEE Trans. Nanobiosci.*, vol. 15, no. 8, pp. 871–880, Dec. 2016.

[20] M. S. Kuran, H. B. Yilmaz, T. Tugcu, and I. F. Akyildiz, "Modulation techniques for communication via diffusion in nanonetworks," in *Proc. IEEE ICC*, June 2011, pp. 1–5.

[21] A. Ahmadzadeh, A. Noel, A. Burkovski, and R. Schober, "Amplify-and-forward relaying in two-hop diffusion-based molecular communication networks," in *Proc. IEEE GLOBECOM*, Dec. 2015, pp. 1–7.

[22] A. P. de Silva *et al.*, "Molecular logic and computing," *Nature Nanotech.*, vol. 2, no. 7, pp. 399–410, Jul. 2007.

[23] P. Siuti, J. Yazbek, and T. K Lu, "Synthetic circuits integrating logic and memory in living cells," *Nature biotechnology*, vol. 31, pp. 448–452, Feb. 2013.

[24] O. Mondragón-Palomino, T. Danino, J. Selimkhanov, L. Tsimring, and J. Hasty, "Entrainment of a population of synthetic genetic oscillators," *Sci.*, vol. 333, no. 6047, pp. 1315–1319, Sep. 2011.

[25] H. ShahMohammadian, G. G. Messier, and S. Magierowski, "Blind synchronization in diffusion-based molecular communication channels," *IEEE Commun. Lett.*, vol. 17, no. 11, pp. 2156–2159, Nov. 2013.

[26] S. Abadal *et al.*, "Bio-inspired synchronization for nanocommunication networks," in *Proc. IEEE GLOBECOM*, Dec. 2011, pp. 1–5.

[27] Y. Lu, M. D. Higgins, and M. S. Leeson, "Comparison of channel coding schemes for molecular communications systems," *IEEE Trans. Commun.*, vol. 63, no. 11, pp. 3991–4001, Nov. 2015.

[28] A. Noel, K. C. Cheung, and R. Schober, "Using dimensional analysis to assess scalability and accuracy in molecular communication," in *Proc. IEEE ICC*, June 2013, pp. 818–823.

[29] M. Pierobon and I. F. Akyildiz, "Diffusion-based noise analysis for molecular communication in nanonetworks," *IEEE Trans. Signal Processing*, vol. 59, no. 6, pp. 2532–2547, Jun. 2011.

[30] R. Mosayebi *et al.*, "Receivers for diffusion-based molecular communication: Exploiting memory and sampling rate," *IEEE J. Select. Areas Commun.*, vol. 32, no. 12, pp. 2368–2380, Dec. 2014.

[31] A. Ahmadzadeh, A. Noel, and R. Schober, "Analysis and design of multi-hop diffusion-based molecular communication networks," *IEEE Trans. Mol. Biol. Multi-Scale Commun.*, vol. 1, no. 2, pp. 144–157, June 2015.

[32] T. N. Cao, N. Zlatanov, P. L. Yeoh, and J. Evans, "Optimal detection interval for absorbing receivers in molecular communication systems with interference," in *Proc. IEEE ICC*, May 2018, pp. 1–7.

[33] N. Tavakkoli, P. Azmi, and N. Mokari, "Optimal positioning of relay node in cooperative molecular communication networks," *IEEE Trans. Commun.*, vol. 65, no. 12, pp. 5293–5304, Dec. 2017.

[34] S. K. Tiwari, T. R. T. Reddy, P. K. Upadhyay, and D. B. Da Costa, "Joint optimization of molecular resource allocation and relay positioning in diffusive nanonetworks," *IEEE Access*, vol. 6, pp. 67 681–67 687, 2018.

[35] A. Noel, K. C. Cheung, and R. Schober, "Joint channel parameter estimation via diffusive molecular communication," *IEEE Trans. Mol. Bio. Multi-Scale Commun.*, vol. 1, no. 1, pp. 4–17, Mar. 2015.

[36] X. Wang, M. D. Higgins, and M. S. Leeson, "Distance estimation schemes for diffusion based molecular communication systems," *IEEE Commun. Lett.*, vol. 19, no. 3, pp. 399–402, March 2015.

[37] S. S. Andrews and D. Bray, "Stochastic simulation of chemical reactions with spatial resolution and single molecule detail," *Physical Biology*, vol. 1, no. 3, pp. 135–151, Aug. 2004.

[38] G. Aminian, H. Ghourchian, A. Gohari, M. Mirmohseni, and M. Nasiri-Kenari, "On the capacity of signal dependent noise channels," in *Proc. IEEE IWCIT*, May 2017, pp. 1–6.

Yuting Fang (S'15) received the B.Eng. degree from Beijing University of Posts and Telecommunications, China, and the same degree with the First Class Honours from Queen Mary University of London, UK, in 2014. She is currently pursuing the Ph.D. degree at the Australian National University, Australia. She was a recipient of the China Scholarship Council scholarship. Her research interests include cooperative molecular communication and behavioral dynamics in microscopic population.

Adam Noel (S'09–M'16) is an Assistant Professor in the School of Engineering at the University of Warwick in Coventry, UK. He received the B.Eng. degree in electrical engineering in 2009 from Memorial University in St. John's, Canada. He received the M.A.Sc. degree in electrical engineering in 2011 and the Ph.D. degree in electrical and computer engineering in 2015, both from the University of British Columbia in Vancouver, Canada. In 2013, he was a Visiting Scientist at the Institute for Digital Communication at Friedrich-Alexander-University in Erlangen, Germany. He has also been a Postdoctoral Fellow at the University of Ottawa and the University of Montreal. His research interests are in the prediction and control of biophysical systems at a microscopic level. Dr. Noel has received several awards from the Natural Sciences and Engineering Council of Canada, including a Postdoctoral Fellowship. He also received a Best Paper Award at the 2016 IEEE International Conference on Communications.

Nan Yang (S'09–M'11–SM'18) received the B.S. degree in electronics from China Agricultural University in 2005, and the M.S. and Ph.D. degrees in electronic engineering from the Beijing Institute of Technology in 2007 and 2011, respectively. He has been with the Research School of Electrical, Energy and Materials Engineering at the Australian National University since July 2014, where he currently works as a Senior Lecturer. Prior to this, he was a Postdoctoral Research Fellow at the University of New South Wales (2012–2014) and a Postdoctoral Research Fellow at the Commonwealth Scientific and Industrial Research Organization (2010–2012). He received the IEEE ComSoc Asia-Pacific Outstanding Young Researcher Award in 2014 and the Best Paper Awards from the IEEE GlobeCOM 2016 and the IEEE VTC 2013-Spring. He also received the Top Editor Award from the Transactions on Emerging Telecommunications Technologies, the Exemplary Reviewer Awards from the IEEE TRANSACTIONS ON COMMUNICATIONS, IEEE WIRELESS COMMUNICATIONS LETTERS, and IEEE COMMUNICATIONS LETTERS, and the Top Reviewer Award from the IEEE TRANSACTIONS ON VEHICULAR TECHNOLOGY from 2012 to 2018. He is currently serving in the Editorial Board of the IEEE TRANSACTIONS ON WIRELESS COMMUNICATIONS, IEEE TRANSACTIONS ON MOLECULAR, BIOLOGICAL, AND MULTI-SCALE COMMUNICATIONS, IEEE TRANSACTIONS ON VEHICULAR TECHNOLOGY, and TRANSACTIONS ON EMERGING TELECOMMUNICATIONS TECHNOLOGIES. His general research interests include massive multi-antenna systems, millimeter wave and terahertz communications, ultra-reliable low latency communications, cyber-physical security, and molecular communications.

Andrew Eckford (M'96—S'99—M'03—SM'15) is an Associate Professor in the Department of Electrical Engineering and Computer Science at York University, Toronto, Ontario. He received the B.Eng. degree from the Royal Military College of Canada in 1996, and the M.A.Sc. and Ph.D. degrees from the University of Toronto in 1999 and 2004, respectively, all in Electrical Engineering. Andrew held postdoctoral fellowships at the University of Notre Dame and the University of Toronto, prior to taking up a faculty position at York in 2006. He has held courtesy appointments at the University of Toronto and Case Western Reserve University; in 2018, he was named a Senior Fellow of Massey College, Toronto. Andrew's research interests include the application of information theory to nonconventional channels and systems, especially the use of molecular and biological means to communicate. Andrew's research has been covered in media including The Economist, The Wall Street Journal, and IEEE Spectrum. His research received the 2015 IET Communications Innovation Award, and was a finalist for the 2014 Bell Labs Prize. Andrew is also a co-author of the textbook Molecular Communication, published by Cambridge University Press.

Rodney A. Kennedy (S'86–M'88–SM'01–F'05) received the B.E. degree (1st class honours and university medal) from the University of New South Wales, Sydney, Australia, the M.E. degree from the University of Newcastle, and the Ph.D. degree from the Australian National University, Canberra. Since 2000 he has been is a Professor in engineering at the Australian National University, Canberra, Australia. He has co-authored close to 400 refereed journal or conference papers and a book "Hilbert Space Methods in Signal Processing" (Cambridge Univ. Press, 2013). He has been a Chief Investigator in a number of Australian Research Council Discovery and Linkage Projects. His research interests include digital signal processing, digital and wireless communications, and acoustical signal processing.